Tasmanian Geological Survey Record UR2017/01

The Caveside flood events of 2011 and 2016: A field investigation and modelling analysis

by *Claire L. Kain, Colin Mazengarb and E. H. (Ted) Rigby*

Department of State Growth

Tasmanian Government

Mineral Resources Tasmania
PO Box 56
Rosny Park Tasmania 7018
Phone (03) 6165 4800
Fax (03) 62338338
Email info@mrt.tas.gov.au
Internet www.mrt.tas.gov.au

August 2017

Authors:
Claire L. Kain (Mineral Resources Tasmania),
Colin Mazengarb (Mineral Resources Tasmania) and
E. H. (Ted) Rigby (Rienco Consulting)

Refer to this document as:
Kain, C. L., Mazengarb, C. and Rigby, E. H. (2017). The Caveside flood events of 2011 and 2016: A field investigation and modelling analysis. Tasmanian Geological Survey Record 2017/01. Mineral Resources Tasmania.

Cover image:
Sediment deposited across the Caveside landscape following the June 2016 flooding. Photograph: Rob Buck (Tasmania Parks and Wildlife Service).

While every care has been taken in the preparation of this report, no warranty is given as to the correctness of the information and no liability is accepted for any statement or opinion or for any error or omission. No reader should act or fail to act on the basis of any material contained herein. Readers should consult professional advisers. As a result the Crown in Right of the State of Tasmania and its employees, contractors and agents expressly disclaim all and any liability (including all liability from or attributable to any negligent or wrongful act or omission) to any persons whatsoever in respect of anything done or omitted to be done by any such person in reliance whether in whole or in part upon any of the material in this report.

Tasmanian Geological Survey Record UR2017/01

The Caveside flood events of 2011 and 2016: A field investigation and modelling analysis

by Claire L. Kain, Colin Mazengarb and E. H. (Ted) Rigby

Mineral Resources Tasmania
Department of State Growth

Tasmanian Government

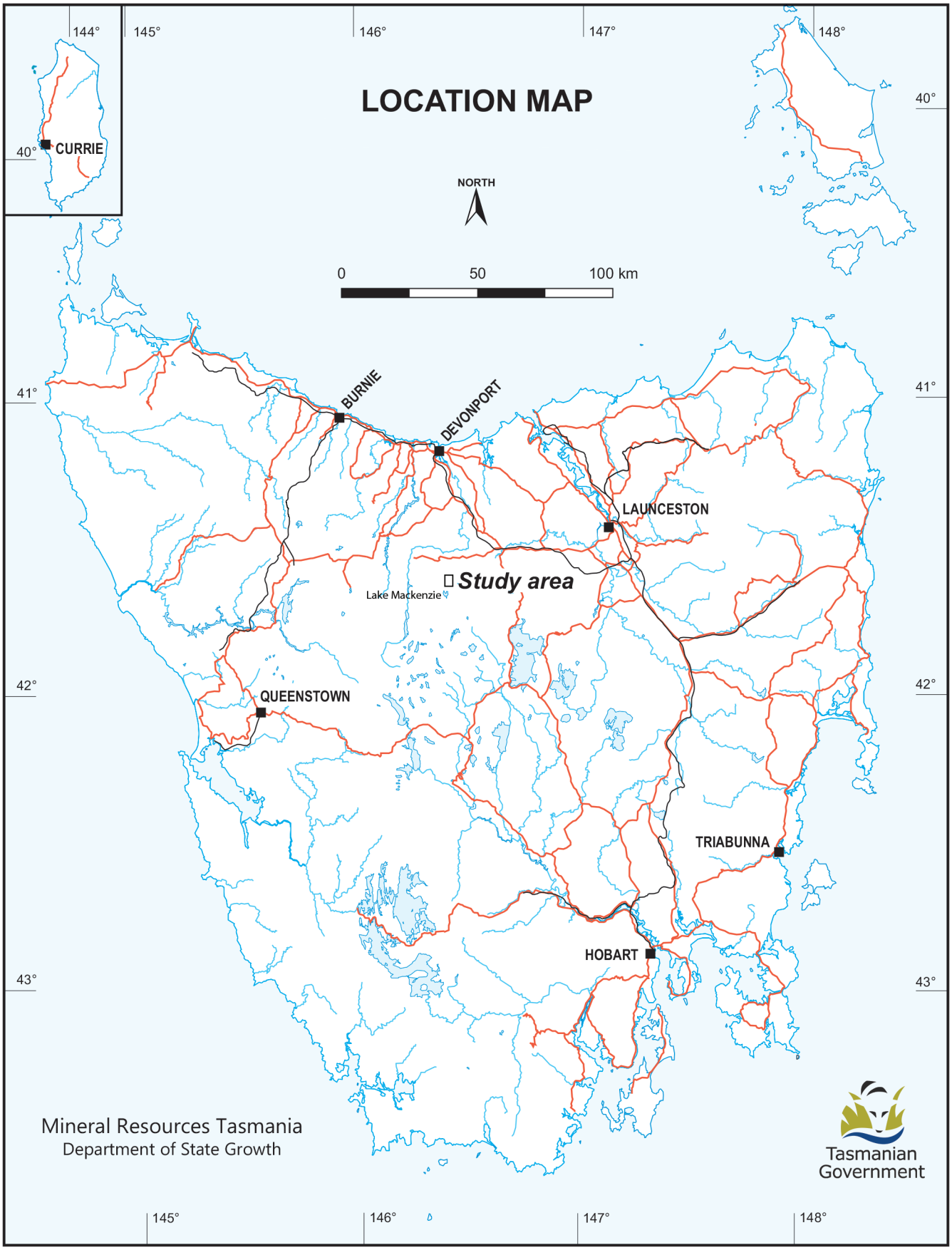
LOCATION MAP
NORTH
0
50
100 km
144°
145°
146°
147°
148°
40°
41°
42°
43°
CURRIE
BURNIE
DEVONPORT
LAUNCESTON
Study area
Lake Mackenzie
QUEENSTOWN
TRIABUNNA
HOBART
Mineral Resources Tasmania
Department of State Growth
Tasmanian Government

Contents

List of figures

List of tables

Executive Summary

Two episodes of intense flooding and sediment transport occurred in the Westmorland Stream system near Caveside, in January 2011 and June 2016. Mineral Resources Tasmania was invited to provide technical assistance to the Tasmanian Flood Recovery Taskforce and DPIPWE who were trying to gain an understanding of these events. Both episodes were initiated by extreme rainfall events (<1% annual exceedance probability for durations exceeding 6 hours) that delivered 300 mm and 400 mm of rainfall, respectively, over a period of several days and had devastating impacts for landowners within the system's alluvial fan. The two events were explored using a combination of field investigations, GIS mapping and hydraulic modelling.

On 14 January 2011, heavy rainfall on the Great Western Tiers escarpment triggered a landslide that transitioned into a debris flow. The runout path of the debris flow was 2.9 km long and up to 50 m wide, and continued flooding deposited gravel, sand and silt across the farmland below. The most intense rainfall occurred over a 12-hour period on 5–6 June, which coincided with the timing of the damage to farmland, and modelling results suggest that peak flood discharge rates reached 55 m^3s^{-1}.

Extreme rainfall between 4 June and 6 June 2016 again caused flooding in Westmorland Stream. The effects included significant deposition of sediment across the alluvial fan and large-scale erosion of the farmland above the fan. Modelling results show that flow velocities reached 4 ms^{-1} and maintained a high (erosional) level for approximately 27 hours. The overall volume of water was also higher during the 2016 flood, reaching a modelled peak discharge rate of 80 m^3s^{-1}.

The impacts of the two events on the farmland were superficially similar; however, this investigation concludes that sediment sources and transport processes differed. The debris flow was a key driver in the 2011 event, and delivered a large volume of sediment downstream to the farmland. In contrast, the impacts in 2016 were caused by an extended period of extreme stream flooding that eroded approximately 5000 m^3 of alluvium from the farmland itself.

These events represent natural processes that occur periodically in this landscape and have contributed to the building of the alluvial fan over many millennia. Statistically, storms of this magnitude have an annual exceedance probability of <1%. As such, the probability of another occurring in the near future is low but not impossible. The geometry of the catchment is also more closely aligned with fluvially dominated fan systems elsewhere, which suggests that flooding represents a more frequent future risk than debris flows. However, ongoing remobilisation in this area or similar locations is a concern for landowners and government managers, particularly in the face of predicted climate change outcomes.

These findings have implications for the economic resilience of the local area and for the physical functioning of the Westmorland Stream system. These floods have altered the morphology of Westmorland Stream, resulting in a wider channel with a decreased response time to smaller floods as well as an increased potential for evaporation and water shortages in dry months. Moreover, an increased flood risk to one farmhouse has been identified, in the case of future flash floods, which may require further investigation and/or mitigation measures.

In a broader context, this situation highlights the need to understand the potential risks from such events in communities around the Great Western Tiers. Further research involving communities, geomorphologists, engineering professionals and local authorities should focus on developing measures to minimise the impacts of future events and build resilience, in case of further flooding.

Introduction

Hydro-geomorphic processes in mountain environments, such as Tasmania's Great Western Tiers (GWT), involve a combination of fluvial, mass movement and other hillslope processes. Extreme flooding, landslides and debris flows have been known to cause problems for property owners and infrastructure managers in such environments. Consequently, an understanding of these processes is important for determining the progression of natural disasters and their impacts, as well as for assessing the probability of and risk from potential future events.

In the past six years, two episodes of extreme rainfall have resulted in intense flooding and sediment movement in the Westmorland Stream system, which comprises a mountain stream and Quaternary alluvial fan. The impacts of both of these episodes were significant for the landowners on the alluvial fan and plains at Caveside, below the GWT. The most recent event occurred in June 2016 and resulted in erosion of the stream bed and the deposition of a large amount of sediment (silt, sand and boulders) across farmland on the alluvial fan. A similar situation occurred in January 2011. Some of the landowners and their families have lived at this location for over 70 years and have not witnessed such severe flooding or debris flows during this time.

Following the severe rainfall event in June 2016, the Tasmanian Flood Recovery Taskforce was established to support the recovery and rebuilding of flood-affected communities. As part of this initiative, Mineral Resources Tasmania (MRT) was invited to assist the Department of Primary Industries, Parks, Water and Environment (DPIPWE) in assessing the extent of the deposition and determining the geomorphic mechanisms of the 2011 and 2016 events. In addition, this investigation also aims to better understand the drivers and functioning of this alluvial fan system on a larger scale, in order to provide some idea of the probability of recurrence and potential risk into the future. These goals were achieved through a combination of field mapping, interpretation of aerial imagery, GIS analysis, and flood modelling. The purpose of the modelling was not only to understand the scour and depositional regimes during these events, but also to deliver a calibrated hydrodynamic model for possible future use. In particular, this model could be useful to investigate the efficacy of any proposed mitigation schemes in the affected area.

This report details the investigation undertaken by MRT at Caveside, including the methodology, scientific results and a conceptual discussion of the geomorphic processes occurring in the Westmorland Stream system. Moreover, the implications of the findings with respect to ongoing land management at Caveside are also considered. Firstly, a background to mountain sediment transport processes is provided.

Fluvial sediment transport and mass movements in mountain environments

The mechanism of sediment transport in mountainous environments is influenced by the slope gradient, the type of material, vegetation cover and the amount of water present. Based on the ratio of solid material to water content, hillslope transport mechanisms exist on a continuum from stream flows to debris avalanches (Fig. 1) and include mass movements, such as landslides and debris flows, and fluvial processes. An understanding of these mechanisms is important for inferring the evolution of the two studied events, as well as for completing a wider interpretation of the Caveside landscape. The differentiation between debris

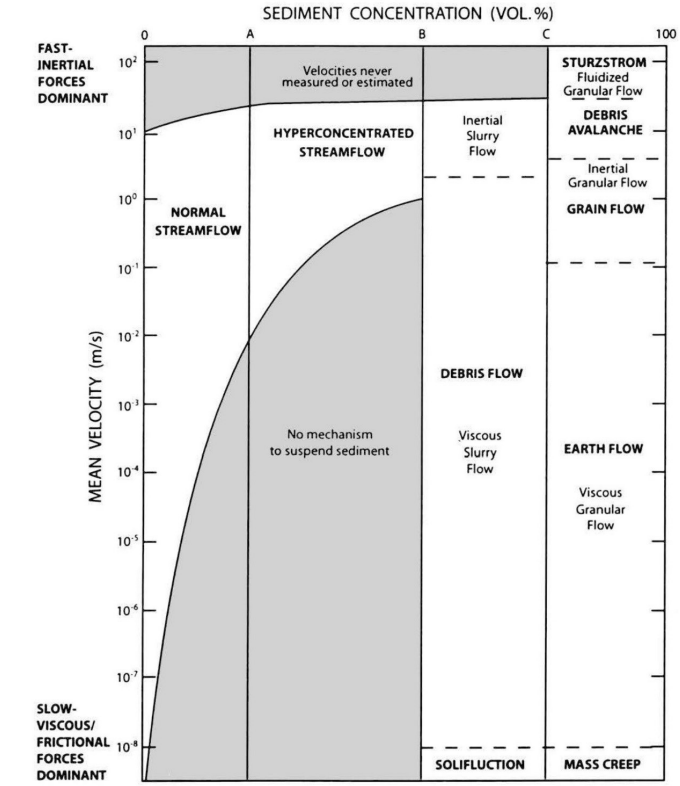

Figure 1. Simplified classification of sediment-water flows, after Pierson and Costa (1987).

flows and stream flooding is of particular importance in the Westmorland Stream catchment.

Debris flows are a form of mass sediment movement that occur in steep environments when sediment is mobilised and transported by water, under the influence of gravity (Takahashi, 2007). They are commonly triggered by heavy rainfall or rapid snowmelt, both of which result in the rapid accumulation of a large volume of water that is capable of destabilising sediments and generating a slurry of water and sediment that travels rapidly downslope. By definition, debris flows have sediment concentrations of above 60% by volume and behave in a plastic manner (Pierson, 2005a). However, the numerical boundaries between flow types are not static and depend ultimately on flow behaviour rather than absolute sediment concentration (Takahashi, 2007; Fig. 1).

The deposits left after a debris flow are generally poorly sorted, contain matrix-supported boulders and may be reverse graded (Costa, 1984). Debris flows transport sediments as a massive, unsorted network of grains, which can allow boulders to be suspended in a matrix of finer sediment and carried further than would be possible by water flow alone. However, the presence of coarse material (cobbles and boulders) alone does not necessarily indicate a debris flow. The toe of a debris flow deposit is often lobate in shape and levees are commonly present at the sides of the transport path (Costa, 1988; Pierson, 2005a). A debris flow event may occur as one or more surges, occurring at intervals of seconds up to hours, with each transporting a slug of sediment (Hungr, 2005).

Hyperconcentrated flows contain approximately 20–60% sediment by volume, and behave in a manner that is intermediate between debris flows (Bingham fluid) and Newtonian stream flows (Pierson, 2005b; Fig. 1). Like debris flows, they are capable of transporting boulders as well as fine material, although in this case boulders are generally transported as bedload. Hyperconcentrated flows may be extremely erosive in steeper channels and tend to cause large-scale aggradation in lower gradient channels. This aggradation then commonly results in lateral channel migration (Pierson, 2005b).

River floods are the most common water-driven sediment transport process, and generally transport less sediment by volume (Fig. 1). For laminar flows, empirical sediment transport relationships have been developed based on flow velocity and particle size (e.g., Hjulström, 1935; Fig. 2). These relationships can be used conceptually to predict whether material will be eroded, transported or deposited, depending on the type of material in the stream bed or alluvial fan and the flow velocity. However, variables such as water depth and bedload transport (particularly important for gravel and boulders) are not accounted for in simple mathematical models and this limitation makes it difficult to back-calculate sediment transport rates for high-energy flows and/or large clasts.

Alluvial fans – Formation and processes

Alluvial fans are cone- or fan-shaped deposits of sediment that occur adjacent to mountain fronts, where streams or debris flows exit a confined area (Allen, 1965; Bull, 1977; Harvey et al., 2005). These fans are part of a sediment erosion and deposition system, whereby sediment is eroded from the mountains and deposited across the fan during flood events. Fan building occurs where the hydraulic geometry of the flow changes as a result of exiting the confined mountain channel. The point of exit is the fan apex, below which the stream channel commonly separates to form a system of braided channels that migrate in response to repeated flooding or changes in sediment load (Bull, 1977; Harvey et al., 2005). The fan surface is distinctly convex in profile, and can be easily identified from aerial imagery and/or topographic mapping, although the outer edge of

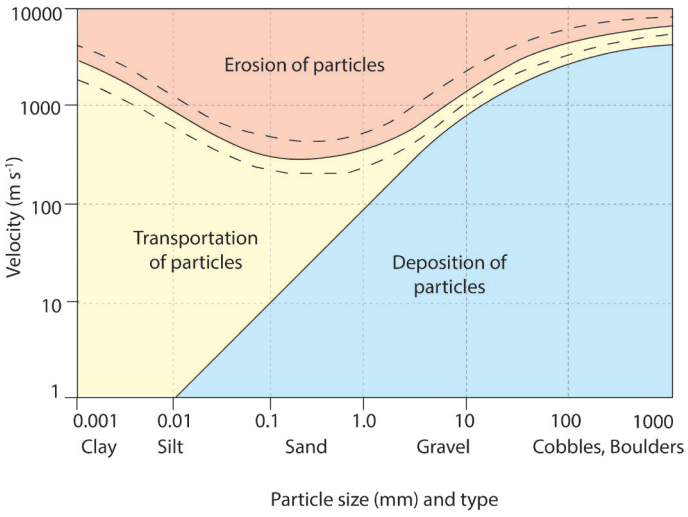

Figure 2. The Hjulström-Sundborg Diagram, which represents critical flow velocity thresholds for sediment erosion and deposition as a function of particle size, modified after Hjulström (1935). This diagram does not account for bedload transport, but still serves a useful illustrative purpose, particularly for understanding the spatial changes in sediment deposition patterns across the alluvial fan and plain.

the fan can be somewhat arbitrary where it grades into the flood plain. A conceptual diagram of an alluvial fan system is presented in Figure 3. It is important to note that an alluvial fan may not be classically symmetrical if constrained on one or more sides by other landforms or fans (Bull, 1977; NRC, 1996).

Alluvial fans may be formed by stream flow, debris flows or a combination of the two processes (NRC, 1996). Moreover, some fans may have been formed by debris flows under different climatic regimes but are now controlled by stream flooding and sedimentation (Bull, 1977). Fans that are fed by both debris flows and flooding are termed 'composite fans' by NRC (1996) and are commonly dominated by lobes and levees in the steeper reaches (debris flow morphology) and divergent flow channels with an apron of finer sediment down-fan (consistent with streamflow deposition).

Accurate identification of the dominant environmental processes is necessary to predict future risk on a given alluvial fan. Previous research has explored differences in the morphometry of fluvially dominated alluvial fans from those primarily formed by debris flows (Crosta and Frattini, 2004; de Scally et al., 2001; 2010; de Scally and Owens 2004; Kostachuk et al., 1986; Santangelo et al., 2012) and, in general, debris flow-dominated systems occur in conjunction with small high-relief basins and flood dominated systems are associated with larger, less rugged watersheds. Other factors that control the basin morphometry and affect the occurrence of debris flows versus fluvial flows include lithology, vegetation type and cover, and land use (Calvache et al., 1997; Lorente et al., 2002; Sorriso-Valvo et al., 1998).

When quantifying the flooding hazard on composite alluvial fans, it can be useful to consider debris flow and stream flood probabilities separately. NRC (1996) point out that a debris flow is not a 'random' event in the same way as a rainfall driven runoff flood, but rather relies on the availability of accumulated debris in conjunction with a triggering event. As such, the average occurrence frequency of debris flows on a fan may not be the same as that of stream floods, and the risk from debris flow events essentially resets to near zero following a major event that strips the source sediment in the catchment (NRC, 1996). Most importantly, the hazard associated with composite alluvial fans relates not only to water inundation, but includes risks associated with sediment erosion and deposition processes that require different consideration and remediation methods than water floods (Davies and McSaveney, 2008; He et al., 2003; Hungr et al., 1984; Jakob and Hungr, 2005). Debris flow fans are considered more hazardous than fluvially dominated fans, due to the higher peak discharge and sediment load associated with debris flows (Hungr et al., 2001; Santangelo et al., 2012; Welsh and Davies, 2011; Wilford et al., 2004).

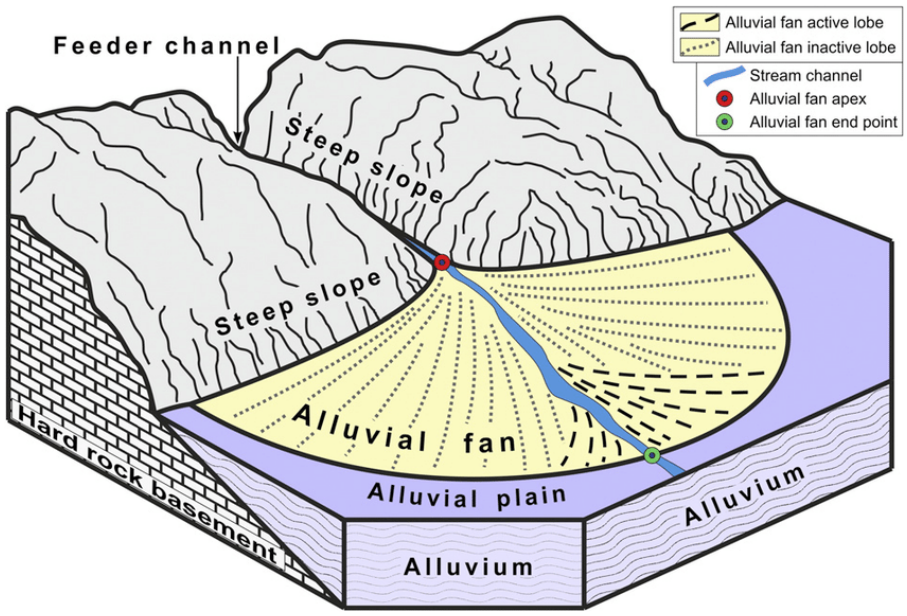

Figure 3. Conceptual model of an alluvial fan system, showing the characteristic shape and relationship between the mountain source area and the depositional fan below. After Norini et al. (2016).

Study Area

Geological setting and land use

The Caveside area lies at the base of the GWT escarpment (Fig. 4), which is located between the central plateau of Tasmania and the lower land of the Meander Valley and northern midlands. The mountain slopes are part of the Great Western Tiers National Heritage Area and Mole Creek Karst National Park, which is forested land that operates largely as a natural system and is managed by the Tasmanian Parks and Wildlife Service. For the purposes of this investigation, the study area is limited to the Westmorland Stream catchment (Fig. 4). Most of the escarpment in this catchment is mature native forest, with a small area of forestry coupes to the east. At the base of the GWT, Westmorland Stream forms an alluvial fan that has been cleared and farmed since the mid to late 1800s.

The best published geology map of the escarpment is that of Jennings and Burns (1958), at a scale of 1:63 360. This map forms the basis of the 1:250 000 statewide geology series produced by MRT. A revised geological map of the study site is presented in Figure 5, which is based on recently acquired LiDAR data and additional field observations. This map makes some simplifications of the stratigraphy for the purposes of the study and the upper parts of the catchment, beyond the elevation of Westmorland Falls, were not investigated.

The escarpment is capped by steep to vertical dolerite bluffs and associated talus (scree) fields. The dolerite sill of Jurassic age overlies shallow-dipping beds of the Permian-Triassic-age Parmeener Supergroup, which comprises sandstone and mudstone dominated lithologies and minor limestone. Other more resistant beds can be identified in the LiDAR imagery. The Parmeener Supergroup unconformably overlies strongly folded Gordon Group Ordovician limestone, which is present near the base of the escarpment. Slopes formed on Parmeener rocks are generally much gentler than the dolerite, but are steepest where underlain by resistant units such as the Ross Sandstone (e.g., Corbett et al., 2014) that occurs in the upper part of the escarpment (Fig. 5). The Gordon Group limestone has a strongly developed karst landscape containing numerous dolines and cave systems, which are controlled by geological structures (folds and faults) that are evident in the LiDAR imagery.

Slope deposits of talus and colluvium mantle much of the escarpment, some of which were previously depicted as Tertiary age boulder deposits on the earlier geological mapping (Jennings and Burns, 1958). In our revision of the geological mapping, we have emphasised the bedrock units rather than the slope deposits. Unvegetated scree/talus deposits are obvious on the dolerite escarpment in the upper catchment and these are depicted later in the flood modelling input data. Despite being widespread, other slope deposits are difficult to map, due to access difficulties and poor exposure outside of stream channels. Several shallow landslides (possibly exceeding 20 in number) are evident along the mid-slope of the escarpment as seen from the road approaching Caveside from Deloraine and on satellite imagery and recent orthophotos accessible from the LIST website and Google Earth. They are visible as areas of bare earth or rock where soil/regolith failures have occurred, removing vegetation. The presence of much larger landslides on the escarpment (within Parmeener rocks) can be inferred from the morphology expressed in recent LiDAR imagery. Some of the landslides discussed have been captured in the MRT landslide database that is publicly viewable. All of this information demonstrates that the area is prone to disturbance from hillslope processes. A small number of large debris flows have also been witnessed on dolerite capped mountains around Tasmania in the years since European settlement (e.g., Anon, 1906).

Hydrology and geomorphology

The escarpment is dissected by a number of incised streams, including Westmorland Stream, which is the focus of this study. Where these streams exit the escarpment they form alluvial fans that transition downstream into low-gradient alluvial flood plains. The formation age of the alluvial lowlands is unknown, although these processes are likely to extend back several million years through the Quaternary glacial periods, as described elsewhere around Tasmania (e.g., McIntosh et al., 2012; Wasson 1977). However, events such as occurred in 2011 and 2016 indicate that they are still forming in contemporary climatic regimes. Most of the streams on the escarpment close to Caveside are currently enclosed in a forest canopy (i.e., the channels are not visible on aerial photographs or satellite imagery); the principal exception being Westmorland Stream.

The alluvial fan in Westmorland Stream is currently farmland, beginning at a point (fan apex) where the channel is no longer constrained by bedrock (Fig. 5).

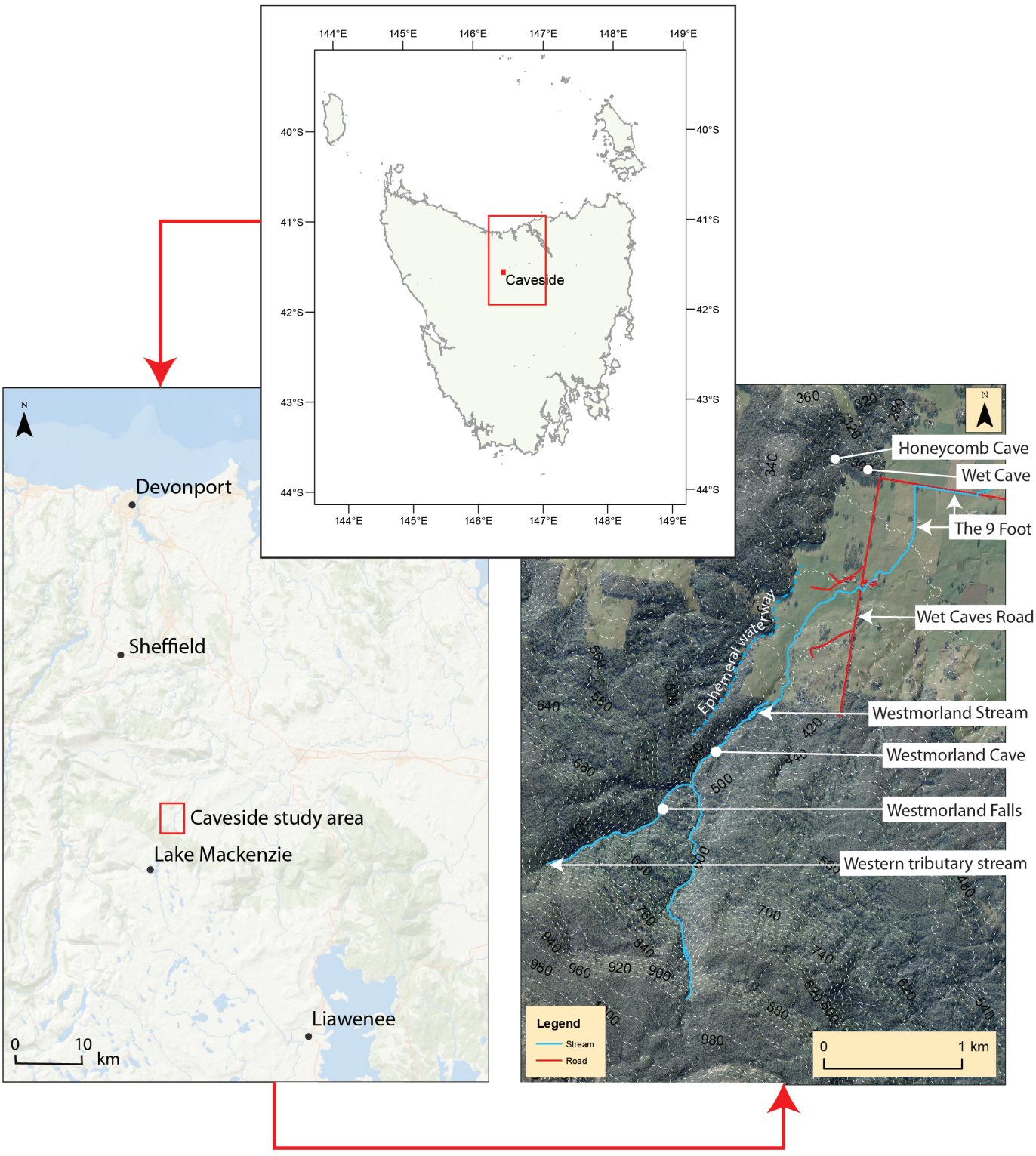

Figure 4. Top: Location of Caveside in Tasmania, Left: Location of rainfall stations. Basemap from ArcGIS online Right: Features of the Caveside landscape mentioned in the text. Base imagery supplied by Meander Valley Council.

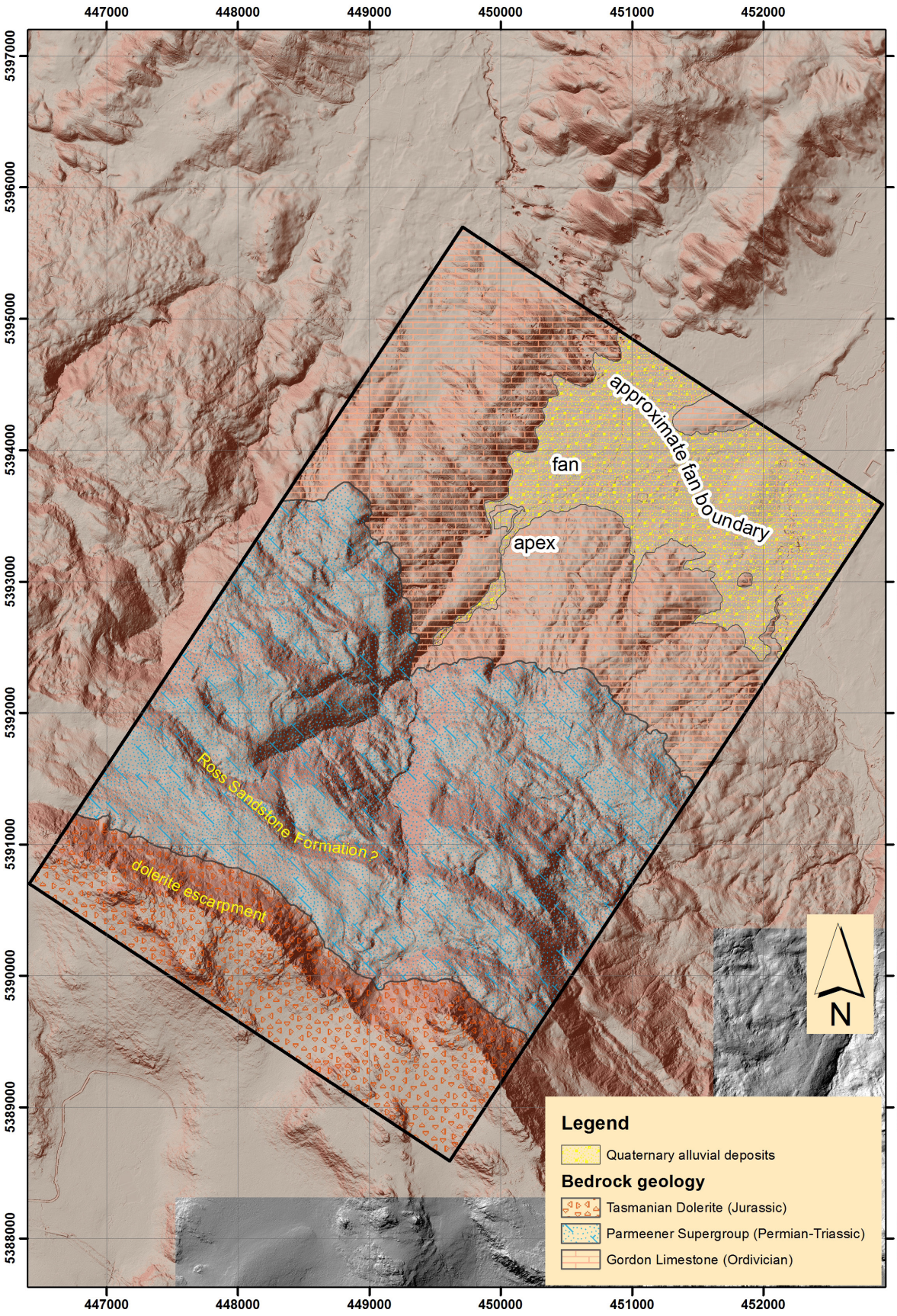

Figure 5. Revised geological map of the study area near Caveside. Hillshade imagery is derived from a publicly available LiDAR dataset commissioned by Meander Valley Council. Map coordinates are Map Grid of Australia (MGA) with grid intervals of 1 km.

The fan is approximately 1.5 km long and up to 1 km wide, and transitions into a flood plain with a poorly defined boundary as depicted in Figure 5. However, the geometry is not classically symmetrical as the fan is bounded to the west by a limestone ridge and coalesces with smaller fans to the east. As visible in Figure 5, the fan/flood plain transition is further complicated by a bedrock high. At the western boundary of the fan, a much smaller stream occurs that appears to be an ephemeral waterway (Figure 4). The path of this stream is constrained by the Westmorland fan in such a way that it hugs the limestone ridge and may lose water to the karst system. LiDAR imagery shows that Westmorland fan is composed of multiple channels with evidence of numerous avulsions as is typical of such features.

The hydrology of the area is additionally complex, due to the karstic environment that interacts with surface flow and rainfall runoff. The wider catchment system includes three limestone caves: Westmorland Cave, Wet Cave and Honeycomb Cave, which are part of the Mole Creek Karst system (e.g., Kiernan, 1995). Westmorland Cave and Wet Cave are located within the Westmorland Stream study area and model domain (Fig. 4), but Honeycomb Cave lies outside this boundary. As a result of the 2011 debris flow, Westmorland Cave became blocked by debris and most of the water that used to flow into the cave now flows down the stream channel (Hunter, 2011).

The modelled catchment area covers approximately 13 km^2 (discussed in the methods section and depicted in Fig. 6). The stream's headwaters are located on scree slopes on dolerite bedrock, at an approximate elevation of 1200 m AHD, with the stream falling to about 300 m AHD at the downstream model boundary. The overall stream length is approximately 7 km, reflecting a relatively steep average stream gradient of about 130 m km^{-1}. Additionally, there are several narrow and steep sided constrictions in the stream's upper reaches.

Anthropogenic modification and management of the stream channel has been ongoing since farming began in the 1800s, in order to ensure a continuous supply of water to the farmland further downstream. In particular, part of the stream has been realigned and several structures have been constructed across the channel in the lower half of the catchment. The realigned channel on the alluvial fan was built by convict labour and is colloquially known as the '9-foot' (Fig. 4). Historically, the stream flow has also been managed by a diversion chute at the entrance to Westmorland Cave, to control the amount of water flowing into the cave and allow a constant supply of water to the pastoral land below.

Methods

Rainfall data

Rainfall data was obtained for Caveside and the surrounding area, covering two periods: 11–16 January 2011 and 4–8 June 2016. These data were obtained from local landowners, the Bureau of Meteorology (BoM, 2016a) and Hydro Tasmania. The Caveside totals were recorded daily at 9 am, by one of the local landowners (located at 41.302°S, 146.416°E). Continuous rainfall records were obtained for Sheffield, Liawenee and Devonport Airport from the Bureau of Meteorology and for Lake Mackenzie from Hydro Tasmania. The locations of these stations in relation to Caveside are shown in Figure 4.

A cumulative rainfall curve was constructed for each location to assess rainfall volumes, along with a set of hyetographs to assess the intensity patterns across the duration of the storm. The volumes and rainfall patterns were compared to those at Caveside and two rainfall stations were selected for further analysis: Lake Mackenzie and Sheffield. Lake Mackenzie is located adjacent to the edge of the Westmorland Stream catchment and is thus particularly relevant. Records from the other two locations were disregarded due to their distance from Caveside and dissimilarity in rainfall volumes. In particular, Liawenee is located 38 km southeast of Caveside and appears to have been sheltered from the direct force of the storms.

Intensity-Frequency-Duration (IFD) curves were constructed for the 2011 and 2016 Lake Mackenzie data and compared to the design IFD data at the same location (extracted from BoM, 2016c).

Field surveys and landscape analysis

Site visits were undertaken on 29–30 August 2016 (approximately 2.5 months after the June 2016 event) and 13–14 September 2016. The landowners presented the damage on their land and described the sequence of events on 6 June 2016. Photographs of the 2016 flood were acquired for the upper part of the farmland, as well as for the area near the base of the alluvial fan. From these photographs, flood depths were estimated. Video footage of the 2011 flood on the farmland above

the alluvial fan apex was obtained from the landowners, and was used to validate flooding patterns and estimate flow velocity where possible. Velocity was estimated from a simple distance/time calculation, whereby the time taken for floating debris to pass between two landmarks was recorded and the horizontal distance measured from the orthophoto in ArcGIS.

A LiDAR survey of the study area was undertaken by local government in 2014 and from these data (LAS file format) a Digital Elevation Model (DEM) was constructed at 1-m resolution, using a linear interpolation algorithm in ArcGIS Desktop software. From the DEM, a slope map was generated and a hydrological basin analysis was undertaken in ArcGIS in order to delineate the boundaries of the Westmorland Stream catchment and determine an appropriate modelling domain. Using the hydrological boundaries and DEM data, seven morphometric parameters were calculated for the Westmorland Stream basin (Table 1) in order to assess the likely dominance of debris flow versus fluvial processes. No comparable data is available for alluvial fans around Tasmania, so the Caveside results were conservatively interpreted with respect to published analyses from alluvial fan systems in cool climates elsewhere (Wilford et al., 2004; de Scally et al., 2010; Santangelo et al., 2012).

The patterns of erosion and deposition were mapped from aerial imagery, for both the 2016 and 2011 events. Oblique aerial photographs of the 2016 damage were commissioned by the Parks and Wildlife Service, Tasmania, immediately following the flood. The images were georeferenced and the approximate extent of deposition and erosion was mapped for the farmland on the alluvial fan using ArcGIS software. These patterns were validated during the second field visit and further areas of deposition added to those mapped from aerial photography; however, it is important to note that the mapped extents represent a minimum record. The dimensions (width, depth, length) of the eroded channel were surveyed in the field, using a basic GPS system (<5 m accuracy), laser range finder and tape measure, and from this the approximate volume of eroded alluvium was calculated. Deposition from the 2011 event was mapped from Google Earth imagery that was acquired in March 2011. Because some clean-up had occurred between January and March 2011, the mapping of the 2011 damage is known to be incomplete.

In addition to mapping debris and flooding downstream, the changes in the national park area were investigated using Google Earth imagery and physical examination of the stream bed. We walked into Westmorland Falls to observe the state of the stream channels along the track and at the falls, and walked downstream along the channel from Westmorland Cave to the farmland boundary.

Table 1. List of morphometric variables used in the landscape analysis.

Morphometric parameter	Derivation	Units
Basin length	Planimetric distance between the fan apex and the furthest point of the watershed boundary	km
Basin area	Planimetric area of the watershed	km^2
Basin inclination	Mean inclination of the watershed	degrees
Fan length	Planimetric distance between the fan apex and the most distant point on the fan surface	km
Fan area	Planimetric area of the alluvial fan	km^2
Fan inclination	Mean inclination of the alluvial fan	degrees
Relief	Elevation difference between the highest and lowest points of the basin	km
Relief Ratio	Basin relief (km) divided by basin length (km)	km/km
Melton Index (Melton, 1965)	Basin relief (km) divided by the square root of basin area (km^2)	km/km
Shape	Basin area (km^2) divided by the square of basin length (km)	km/km

After de Scally et al. (2010) and Wilford et al. (2004).

Modelling using RiverFlow-2D

Model selection

A two dimensional (2D) model was required to replicate the temporally variable and braided nature of the flow on the alluvial fan, and Riverflow-2D (Hydronia, 2016) was chosen for this study. Riverflow-2D is an unstructured mesh, finite volume based model with the ability to incorporate detailed model topography, spatial variability in surface roughness and spatial variability in rainfall and losses. The Surface Water Modelling System (SMS) software developed by Aquaevo was used to both pre-process the input data for use by Riverflow-2D and to post-process the results of each simulation, as per the methods outlined by Hydronia (2016).

Model construction

The model domain was set to incorporate the catchment extent shown in Figure 6. The inputs included the aforementioned 1 m DEM, a Manning's Roughness layer, and rainfall data for the duration of each event. The daily rainfall volume obtained for Caveside was compared against daily volumes for Sheffield (to the north) and Lake Mackenzie (on top of the GWT to the south). The pattern of intensities was consistent for these two locations, so it was possible to construct a rainfall gradient between the two that passed through Caveside and accounted for orographic rainfall effects across the modelled catchment. This was achieved by interpolating between the Lake Mackenzie and Sheffield pluviometer stations using a scaling factor that aligned with the daily records obtained from Caveside.

Input data was mostly generated in shapefiles or ASCII grid format and used to construct a generic unstructured grid model in Aquaveo SMS, which was in turn converted into Riverflow-2D specific format when Riverflow-2D was executed. Three levels of mesh resolution were applied in the model to reflect the required computational accuracy. The stream channel was meshed with 2 m triangles so that the stream cross section and within bank hydraulics could be reasonably simulated. The adjacent floodplain was meshed with 5 m triangles, as this area is not as topographically variable as the stream. However, the mesh size needed to be reasonably small so that the hydraulics of the braided flow could be realistically simulated. The

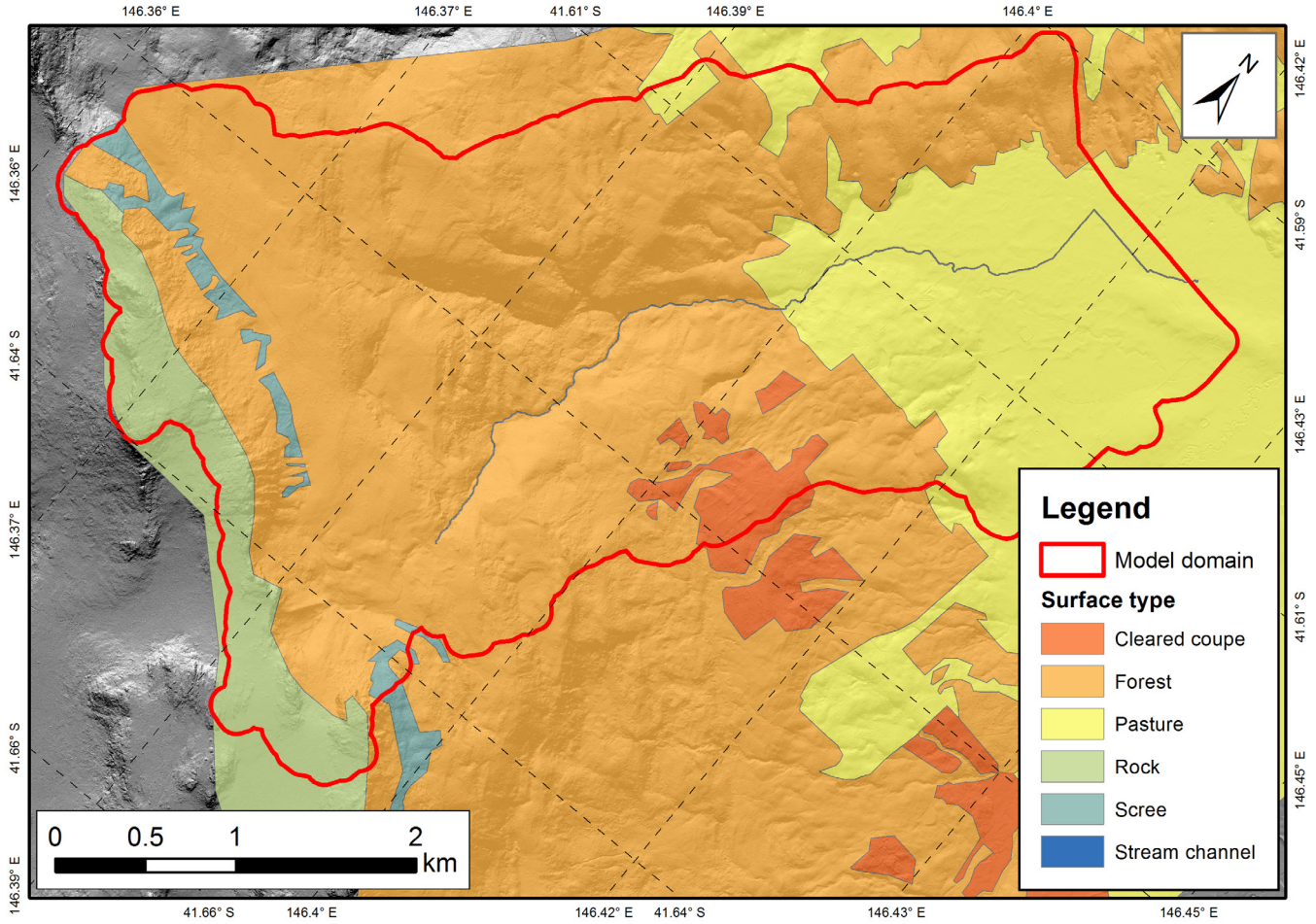

Figure 6. Map of surface type zones in the study area. Manning's *n* values were applied to the model domain according to surface type with values as listed in Table 2.

remainder of the modelled catchment area was meshed with 20 m triangles as this residual area only needed to adequately represent the hydrologic processes involved in the conversion of rainfall into runoff and the mesh could therefore be much coarser. Elevations were then applied to the mesh nodes from the DEM.

The Manning's Roughness layer represents spatial variation in surface friction, which affects how water will flow across the landscape. This layer was manually digitised from aerial imagery, with roughness values assigned according to land cover type (i.e., scree, forest, pasture, river channel). Surface roughness was assigned to the model domain from a shapefile in which the domain had been divided into seven zones as shown in Figure 6. The selected Manning's *n* for each zone is given in Table 2.

While some small culverts and bridges were present in the modelled area prior to each event, they were either destroyed or blocked by debris during these events and have not therefore been included. As the DEM reflects the levels of the roads over these structures, the constructed models reflect an 'all structures blocked' scenario. Moreover, as the actual flood levels at the downstream model boundary are not known, a free (normal) flow surface elevation was adopted as the model's boundary condition based on a flood surface gradient downstream of the model boundary set at 1:500. The main flow bifurcates around a high knoll prior to reaching the downstream model boundary, so this condition was applied either side of the knoll.

Rainfall was applied directly to the model with the Lake Mackenzie rainfall (2016 and 2011) applied to the upper half of the catchment and a synthesized rainfall to the lower half of the catchment formed by scaling the Lake Mackenzie rainfall as previously described. Flood simulations were then run for both the 2011 and 2016 events.

Table 2. Manning's *n* coefficients applied for the differing surface-cover types in the catchment.

Zone	Manning's *n*
Stream waterway – Lower half	0.045
Stream waterway – Upper half	0.060
Pasture	0.050
Bare rock	0.050
Cleared coupe	0.070
Forest	0.100
Scree slopes	0.150

See Figure 6 for the spatial distribution of each land-cover type.

Calibration and sensitivity analysis

The flow depths for 2016 were calibrated against depths estimated at 24 locations from geotagged ground photographs. The DEM at each location was then used to establish the associated flood elevation. Differences in modelled and observed depths were investigated through a sensitivity analysis, whereby the 2016 flooding scenario was re-run using only the Lake Mackenzie rainfall (i.e., a higher rainfall volume) to assess the impact of different rainfall volumes on simulated flood depths. The fit achieved by this calibration process is discussed in the "January 2011" section on page 27.

Community meeting

At the conclusion of the scientific investigation, a community meeting was arranged to present the findings and receive feedback from the Caveside community and local government representatives. This meeting took place on the evening of 7 December 2016. Following our presentation, the community discussed management options informed by the study findings.

Results

Basin and fan morphometry

The morphometric parameters of the Caveside alluvial system are summarised in Table 3, alongside mean values from published literature in similar settings. The watershed encompasses an area of 6.67 km^2 and the boundaries (determined from hydrological analysis and separate from the modelling domain) are outlined in Figure 3. The basin relief (from the top of the escarpment to the fan apex) is 0.86 km with a variable gradient (Figs 7 and 8), reaching a maximum of >70° at the top of the dolerite escarpment. However, most of the basin is less steep, with a mean inclination of 17° and only 9.6% of the basin exhibits a slope greater than 30° (Figs 7 and 8). In contrast, the mean fan inclination is 3.9°.

June 2016

Rainfall

The flooding that occurred in Caveside was part of wider-scale rainfall and flooding that occurred throughout eastern Australia, due to the formation of an East Coast Low weather system in the Tasman

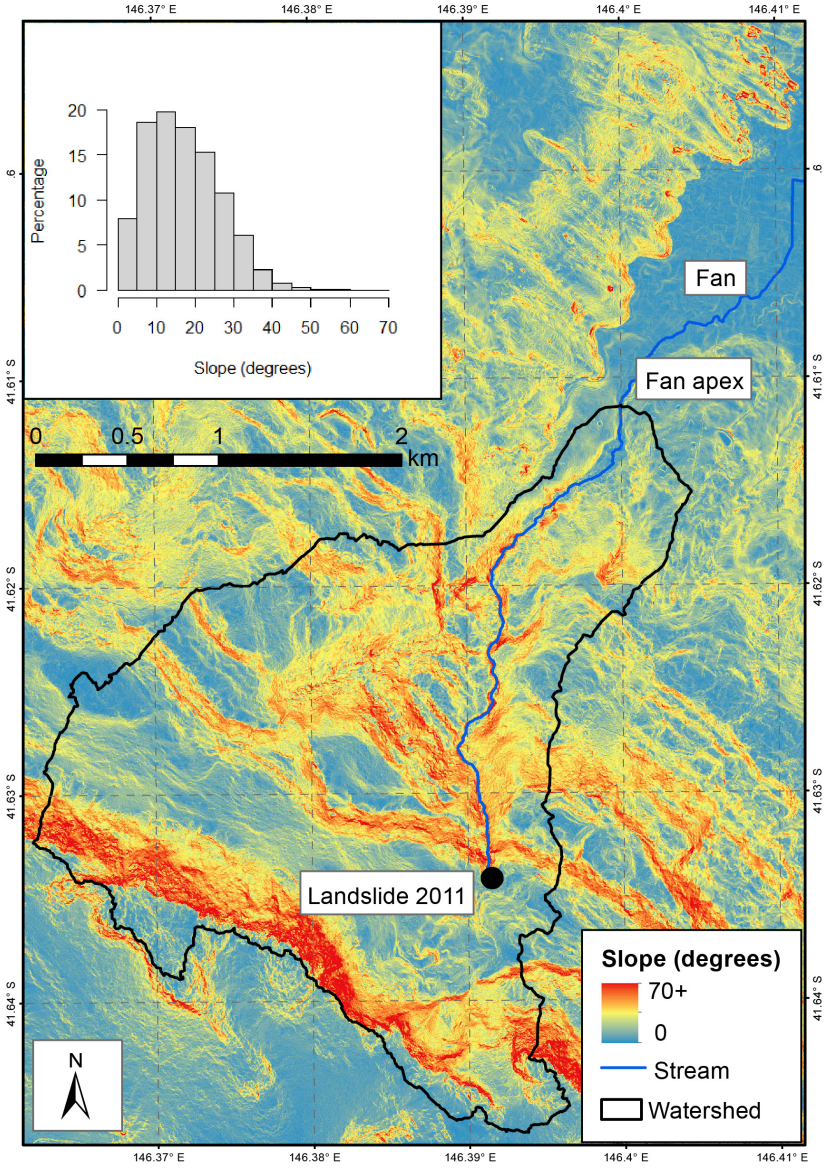

Figure 7. Slope map of the catchment basin, with areas of low slope in blue and high slope in orange and red.

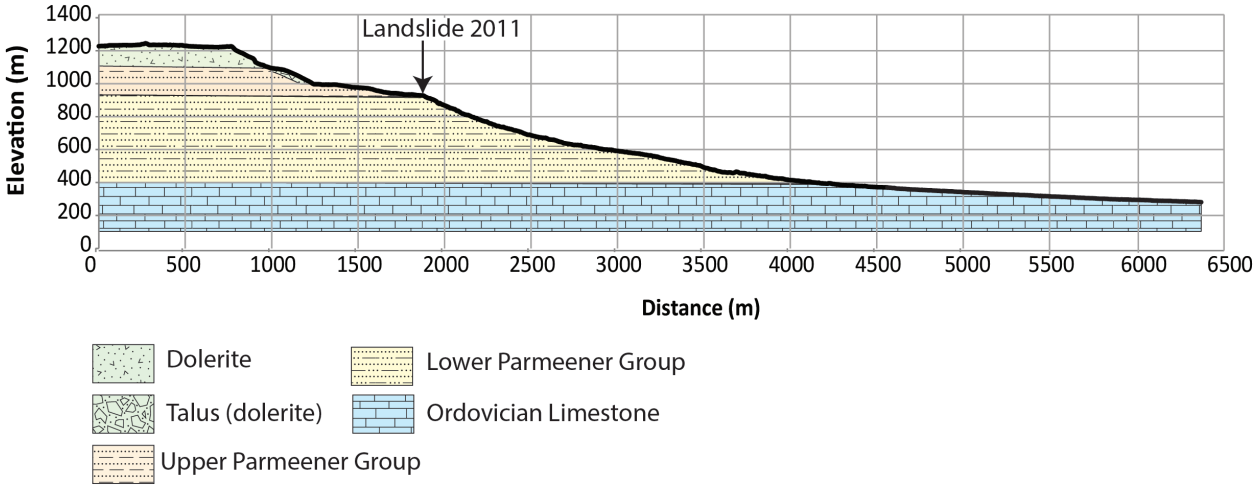

Figure 8. Cross section of the basin and fan, following the path of Westmorland Stream, as depicted in Figure 4.

Table 3. Morphometric parameters for the Caveside alluvial system, compared with mean values for alluvial fans in mountain systems elsewhere in the world, taken from existing literature.

	Caveside	Wilford et al. (2004): Mean (SD)	de Scally et al. (2010): Mean (SD)	Santangelo et al. (2012): Median
Basin length (km)	3.89			
DF[1]		2.06 (1.00)	2.77 (0.89)	1.1
FF[2]		8.9 (4.83)	6.67 (3.41)	3
HF[3]		4.4 (1.92)	NA	NA
Basin area (km²)	6.67			
DF		1.3 (1.1)	3.14 (2.63)	0.42
FF		34.3 (31.4)	23.21 (23.77)	2.7
HF		7 (6.7)	NA	NA
Fan area (km²)	0.71			
DF		NA	0.523 (0.544)	0.11
FF		NA	1.284 (1.408)	1.36
HF		NA	NA	NA
Fan inclination (°)	3.9			
DF		NA	6.7 (3.8)	8.62
FF		NA	1.4 (0.9)	5.86
HF		NA	NA	NA
Relief (km)	0.86			
DF		1 (0.4)	1.354 (0.387)	0.59
FF		1.1 (0.6)	1.308 (0.530)	0.78
HF		1.2 (0.3)	NA	NA
Melton Index	0.33			
DF		0.95 (0.19)	0.94 (0.35)	1.19
FF		0.23 (0.1)	0.35 (0.15)	0.61
HF		0.57 (0.26)	NA	NA
Relief ratio	0.22			
DF		0.49 (0.11)	0.51 (0.15)	NA
FF		0.12 (0.06)	0.22 (0.07)	NA
HF		0.3 (0.11)	NA	NA

[1] DF - the average values reported for debris flow fans.
[2] HF - the average values reported for those dominated by hyperconcentrated flow.
[3] FF - the average values reported for fluvial fans.

Sea. This system had a particularly severe impact in northern Tasmania, where it interacted with other low pressure systems and caused a moist north-easterly airflow that delivered extreme rainfall to much of the state on the 5–6 June 2016 (BoM, 2016b). Flooding was extensive and continued for several days following the rainfall. A plot of total event rainfall (Fig. 9a) shows the Westmorland Stream located in the centre of the highest rainfall zone in north-western Tasmania.

At a Caveside farm house (41.602°S, 146.416°E), a cumulative rainfall total of 286 mm was recorded between 4 June and 7 June. This record represents daily readings of a local rainfall gauge. Records from surrounding pluviometers demonstrate a significant orographic rainfall effect, with the highest precipitation totals and intensities recorded near the northern edge of the GWT (Fig. 9). Lake Mackenzie received the highest rainfall of the gauges surveyed (including others on the GWT), reaching a cumulative total of almost 400 mm between 4 June and 7 June. A hyetograph showed the event involved several identifiable bursts over a two day period, with the majority of this rain falling in a 29-hour period between 4 am on 5 June and 9 am on 6 June (Fig. 9b). At Lake Mackenzie, rainfall intensity peaked at 35 mm hr^{-1} at 4 pm on 5 June. Rainfall volumes were lower on the plains below the GWT, but followed the same temporal pattern. On the plains, the Sheffield School pluviometer provides the closest continuous rainfall record to Caveside, and the data obtained here agrees well with the Caveside daily records and with the pattern of the Lake Mackenzie data (Fig. 9c).

When compared with the BoM Intensity-Frequency-Duration (IFD) data for Lake Mackenzie (Fig. 10), it can be seen that for shorter duration rainfall, burst intensities were not rare, but were less common as the burst duration exceeds 1 hour. It is not clear what the

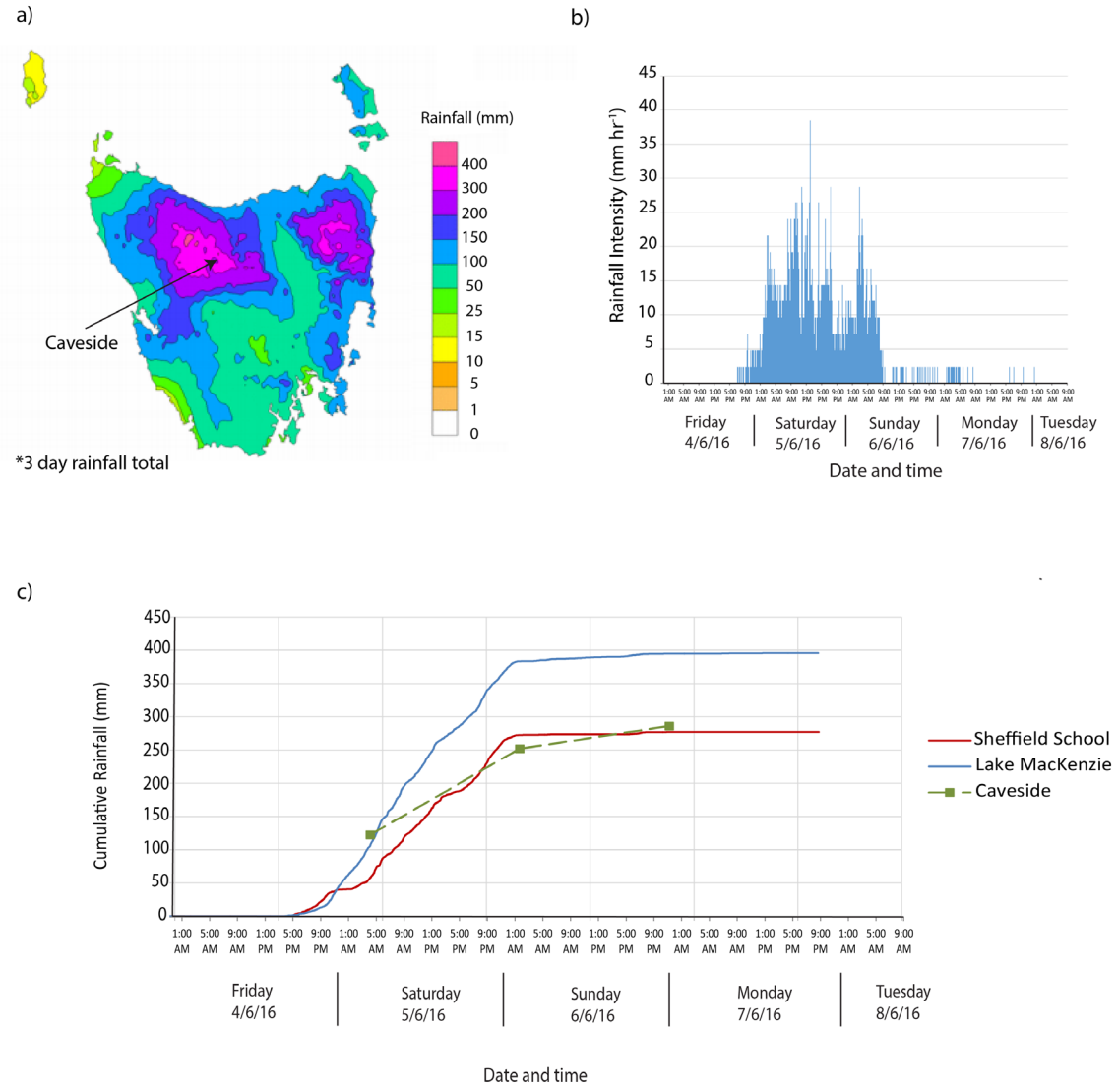

Figure 9. Rainfall data for the June 2016 storm. (a) 3-day rainfall total across Tasmania (BoM, 2016b), showing the location of Caveside in an area of maximum rainfall; (b) hyetograph of rainfall at Lake Mackenzie, on the GWT above Caveside; (c) cumulative rainfall at Caveside (daily totals) and the two rainfall stations nearby (continuous data).

Annual Exceedance Probability (AEP) of the 6–48-hours duration bursts would be, as the current BoM IFD data only includes Annual Exceedance Probabilities (AEPs) up to the 1% (1:100) level. Beyond 6-hours duration, the event rises above the 1:100 AEP line. However, it is apparent from the graph that rainfall in this longer duration burst range, from 6–48 hours, was extremely rare. The BoM rainfall gauge 91016, at Caveside, operating between 1906 and 1988, shows no other comparable events to those of 2011 and 2016 (using 3-day running totals). The highest 3-day total in this period was 160 mm. This result is consistent with the accounts of the local landowners, some of whom have lived in the area for about 70 years.

Landslides on the tiers above Caveside

A number of landslides were initiated by the storm, and can be seen from the roads below and in Google Earth imagery acquired in late 2016 (mapped in Fig. 11). These landslides have been recorded in MRT's landslide database (IDs 6341-6344 and 6346-6355). Larger landslides are concentrated along the geological boundary between the upper and lower Parmeener Supergroup rocks (in the vicinity of the Ross Sandstone), which manifests in the landscape as an escarpment-forming ridgeline and break in slope (Figs 5 and 7). However, many smaller landslides were also mapped lower down the slopes of the Westmorland Stream catchment. Despite the large number of new landslides identified, none of these feed directly into Westmorland

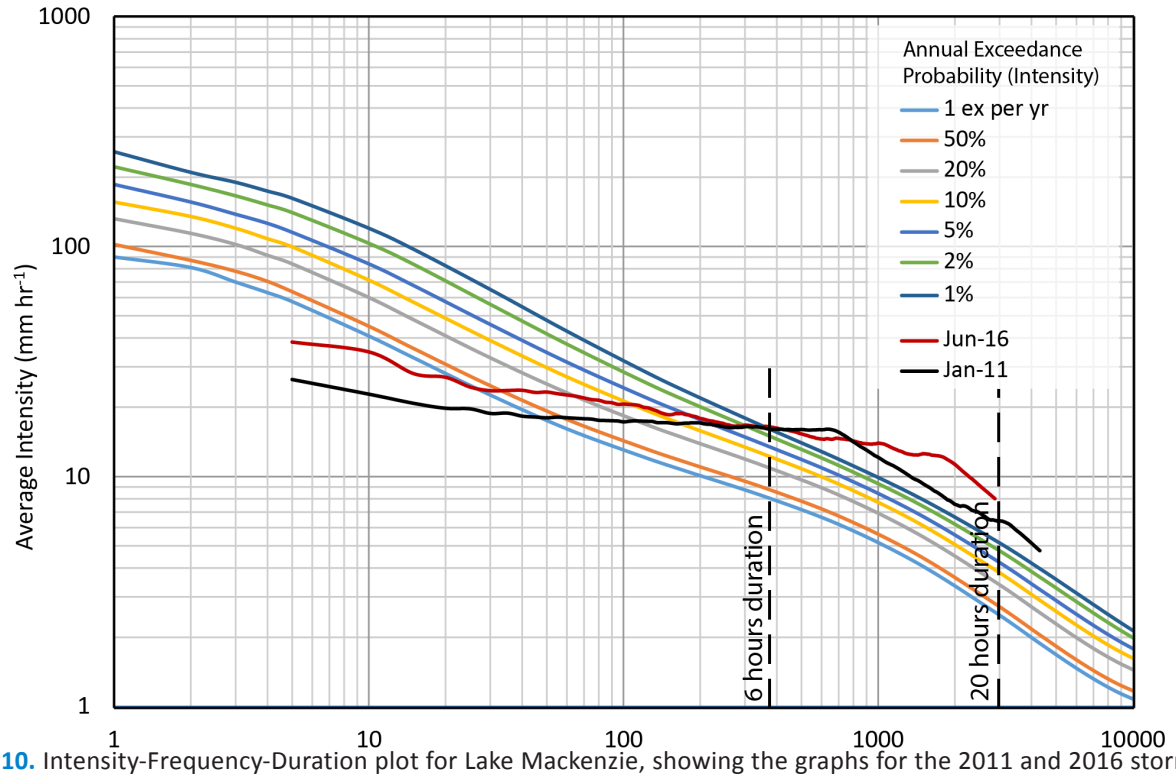

Figure 10. Intensity-Frequency-Duration plot for Lake Mackenzie, showing the graphs for the 2011 and 2016 storms compared with curves associated with key exceedance probabilities. Data obtained from BoM (2016c).

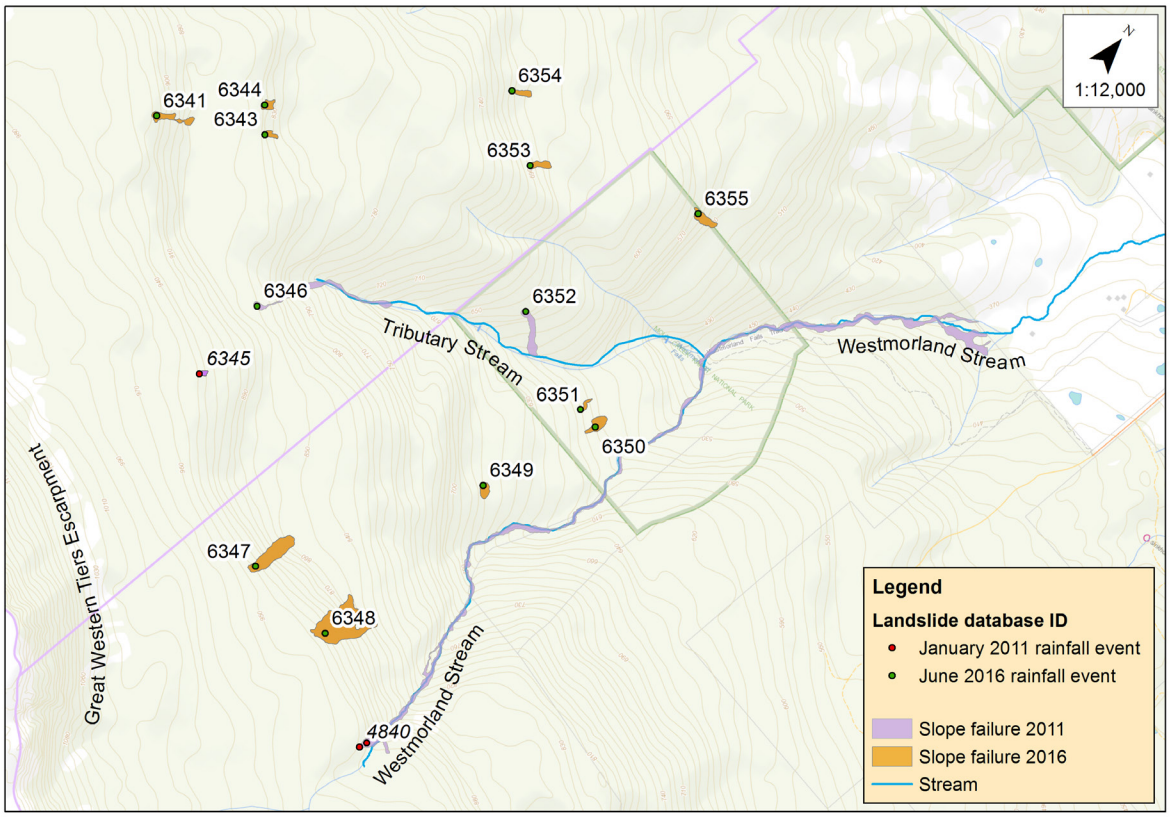

Figure 11. Map of slope failures on the slopes above Caveside following the 2011 and 2016 storms. Slope failures are labelled with their MRT landslide database identification number and coloured according to event: 2011 = purple and 2016 = orange. Base map from ArcGIS online, with a contour interval of 10 m.

Stream. However, two are associated with the tributary stream that feeds into Westmorland Stream and on which Westmorland Falls is located (Fig. 11). A small landslide is visible at the head of the tributary stream and the stream bed has been scoured down to the confluence with Westmorland Stream. Another appears to feed into the tributary stream approximately 500 m above the confluence between the two streams.

Observations and patterns of erosion and deposition

Initial flooding at Caveside occurred overnight on 5–6 June, before a pulse of debris deposition followed at 2:30 pm on 6 June (Ruth Linger, pers. comm. 30 August 2016). Stream flooding continued for three days. Patterns of erosion and deposition across the pasture are shown in Figure 12.

The impacts on the hillside channel (upstream of the farmland) were difficult to identify and separate from the remnants of damage wrought by the 2011 event. The bridge across Westmorland Stream was destroyed by the 2011 debris flow and has been replaced at a height of 2 m above the stream bed. At this point, the stream flows directly over bedrock (Parmeener Supergroup mudstone), although boulders and woody debris were observed both upstream and downstream of this location. The stream bed was open and boulder-filled, but limestone bedrock was exposed near the entrance to Westmorland Cave. The cave entrance was blocked by a large collection of logs and woody debris.

At Westmorland Falls (on the western tributary stream that joins Westmorland Stream; Fig. 4), a viewing platform had been destroyed by the June 2016 flood and a comparison of field observations and photographs from 2013 show that significant vegetation stripping and morphological change occurred during this event. At the time of the field survey, the stream bed was composed largely of boulders and cobbles, but photographs taken prior to 2016 show a low-energy environment with a sandy bed infilled between boulders and delicate overhanging vegetation. Deposits of gravel and boulders, as well as a large log-jam, were also present at the confluence of the falls stream and Westmorland Stream as of September 2016.

On the farmland immediately above the alluvial fan apex, evidence of both erosion and deposition

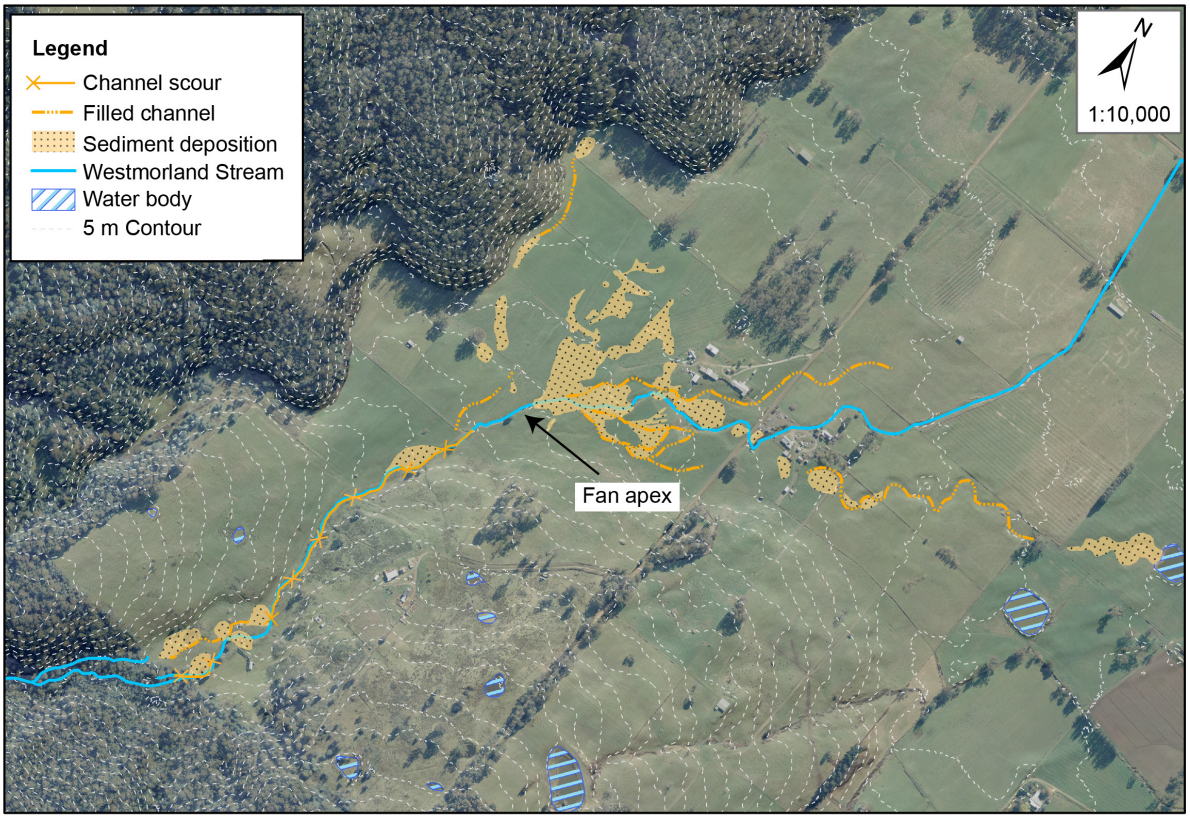

Figure 12. Patterns of erosion and deposition across the pasture in June 2016, mapped from aerial imagery and field validation visits.

was observed. In contrast to the land below, the sedimentary signatures here had not been artificially modified at the time of our field visits. Deposits near the boundary of the national park were very poorly sorted and commonly contained boulders supported by a matrix of silts and sands (Fig. 13). Levee structures were also observed inside the forest boundary, with a toe-shaped deposit extending beyond the park onto the farmland. The stream bed channel below these deposits was deeply scoured in two general areas and a second, smaller, eroded channel appeared at the NW margin of the valley floor. At one location, the original stream channel became infilled with sediment and the flood cut a new channel to a depth of 1.5 m through the paddock (Figs 12 and 13). The two zones of channel erosion (measuring approximately 100 and 300 m in length, respectively) were separated by a large area of boulder deposition. Within the deeply eroded channels (maximum depth 2 m), the stratigraphy showed layers of sub-angular–rounded boulders and gravel, interspersed with soils. Sediment was deposited alongside the upstream erosional zone, and ranged in size from sand to boulders. In particular, a lobe of comparatively finer material (predominantly sand and gravel) was deposited in the NW part of the area. No sediment deposits surrounded the 300-m scour zone, but evidence of flooding was present in the destruction of fences and the presence of vegetation debris trapped in the fence wire. The depth of the channel gradually decreased along this zone, before entering another, smaller, area of deposition where the stream exits a confined zone between two hillsides. This topographic change can be clearly seen in the slope map in Figure 7. The approximate volume of the scoured zone was calculated to be >3500 m^3.

In the central part of the alluvial fan, large amounts of sediment (boulders and sand) were deposited (Figs 12 and 13). Fine sediment and boulders were deposited across the land on either side of the stream channel and the channel was infilled by material. In some cases, fences were destroyed or acted as sediment traps that constrained the boulders and gravel. At the time of the field visits, this material had been consolidated into large piles using earthmoving equipment and the stream channel had been excavated. The landowner's son (acting as an earth-moving contractor) estimates that 4000–5000 tonnes of material was deposited in this area during the event (Mick Linger, pers. comm. 15 September 2016).

Severe flooding and silt deposition occurred across the lower part of the alluvial fan and the flood plain downstream. Flooding in these lower reaches was potentially exacerbated by the addition of water that was exiting the karst system at Wet Cave corner (Fig. 4). A local witness recalls the water pouring from the entrance to Wet Cave in a pressurised jet (Sally Martin, pers. comm. 14 September 2016).

In the months following the 2016 flooding and the excavation of filled parts of the channel, landowners report that the widening of the stream bed has caused the system to respond faster to rainfall inputs of a smaller magnitude (Noel Martin and Rodney Linger, pers. comm. 7 December 2016). In other parts of the stream bed, slugs of silt have continued to move downstream, causing infilling of the 9-foot and overflow during smaller events.

Flood modelling and field validation

The outflow hydrograph from the 2016 model (Fig. 14) shows that the June 2016 event involved several pulses of high flow during the first 36 hours. When the resulting velocities are viewed throughout the event, pulses of high velocities associated with these flow peaks are apparent, and exceed 4 ms^{-1} in some locations. The pattern of maximum velocities across the catchment shown in Figure 14 is repeated, at slightly diminished levels and plan extents, several times during the event. A peak simulated discharge rate of 80 m^3s^{-1} was recorded at the downstream model boundary.

The results of the flood modelling are consistent with observations from field visits and aerial photograph mapping. The modelled flood was tightly constrained in the upper part of the alluvial fan and spread out to form a braided pattern across the flood plain below (Fig. 14). Velocities were low near the top of the escarpment and progressively increased down Westmorland Stream. The area of highest velocity flow matches the locations of the scoured channels mapped in the field (Fig. 14) and the areas of decreasing flow velocity correspond with the mapped areas of deposition. Moreover, mapping of the flooding margins around the deposition zone matches well with modelled flooding extents.

The tabular comparison of modelled and estimated peak flood levels (Table 4) showed modelled depths were consistently lower than observed flood depths, particularly on the farmland above the alluvial fan apex. However, although all simulated levels are less than those estimated, they are for the most part within

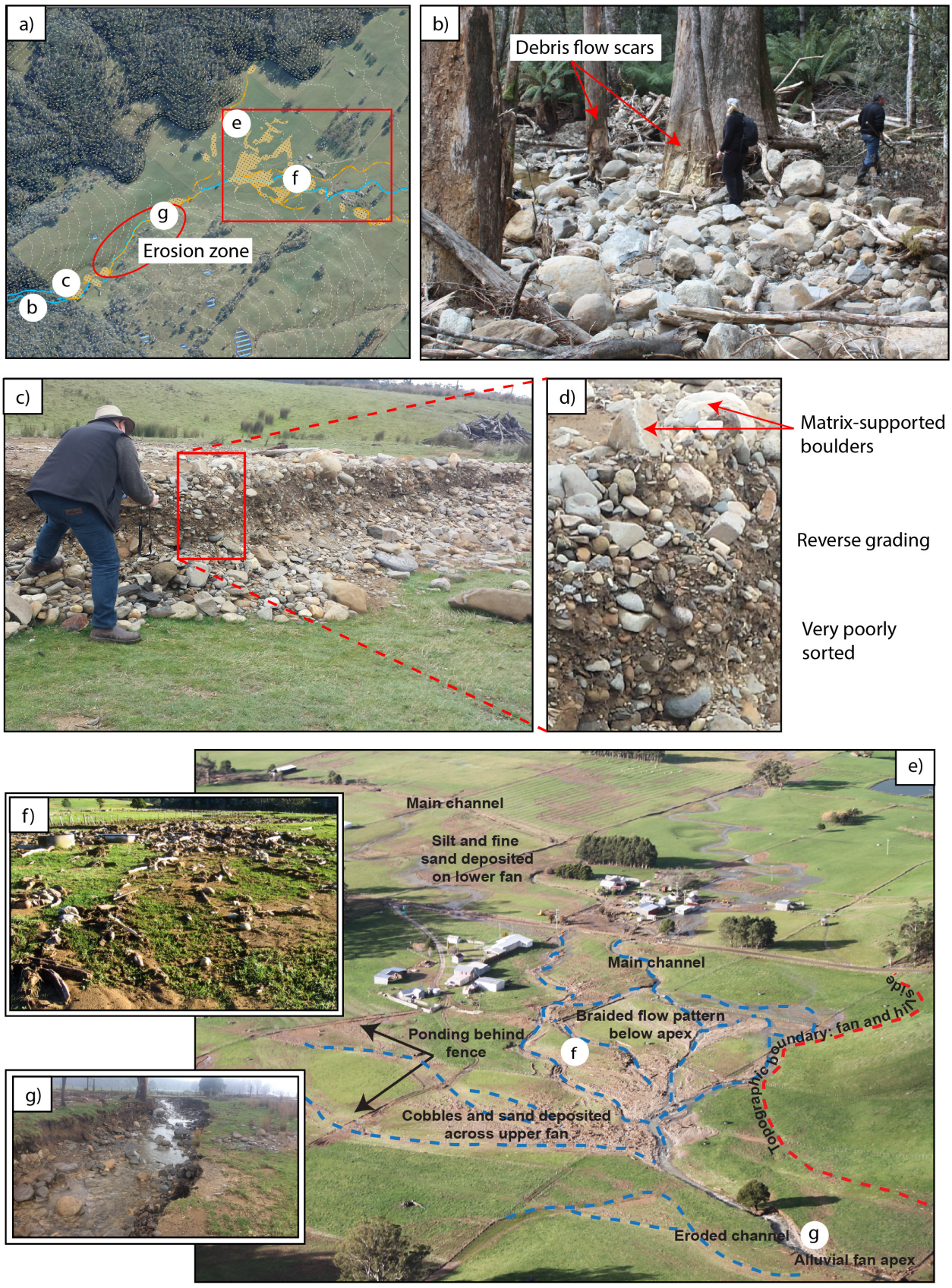

Figure 13. Photographs of deposition and erosion following the June 2016 event. (a) Locations of photographs with respect to the mapped impacts; (b) debris flow deposit and scars near the forest boundary. NOTE: It is unknown whether these scars relate to 2011 or 2016; (c) debris flow deposits at the upper part of the farmland, following the 2016 event; (d) close up of the debris flow deposit stratigraphy and defining characteristics; (e) annotated aerial image of the alluvial fan in the days immediately following the 2016 flood; (f) example of the flood deposits on the mid-lower part of the alluvial fan; (g) part of the eroded channel, at the fan apex.

a) Simulated flooding extent

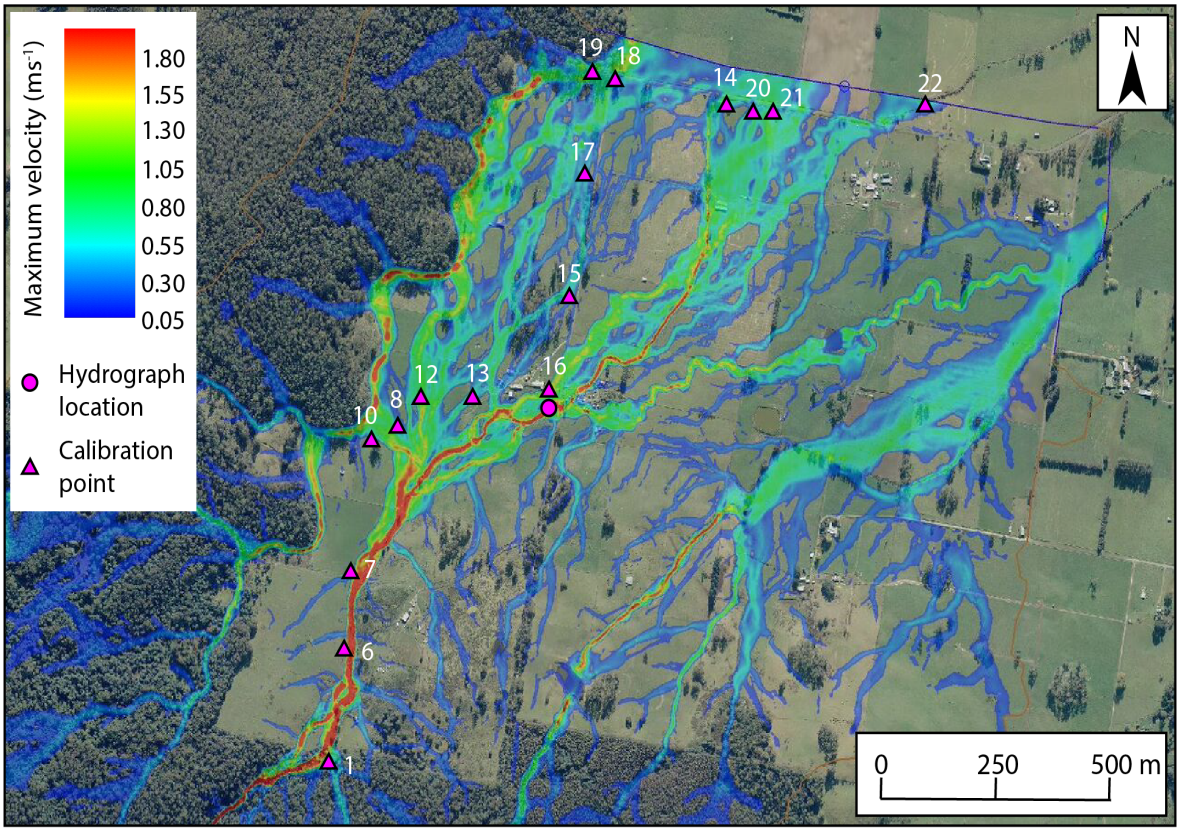

b) Outflow hydrograph

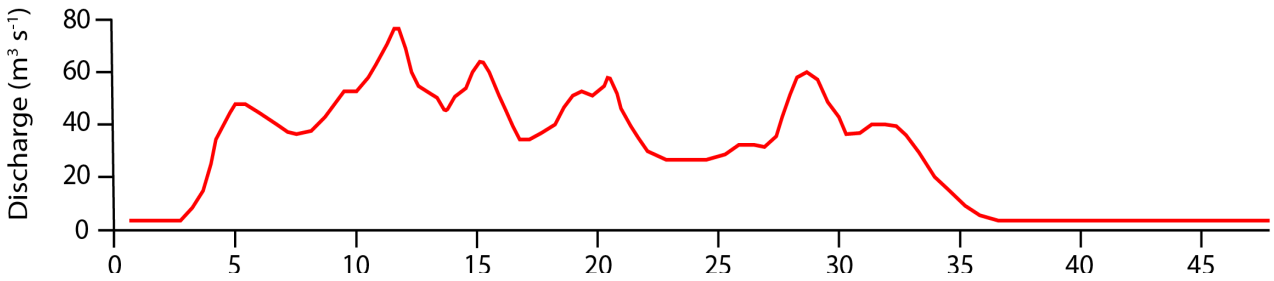

Figure 14. Results of hydraulic modelling for the 2016 event. (a) Flooding patterns and maximum velocities across the pasture and alluvial fan; (b) outflow hydrograph, showing modelled flood elevations in the Westmorland Stream channel near the base of the alluvial fan.

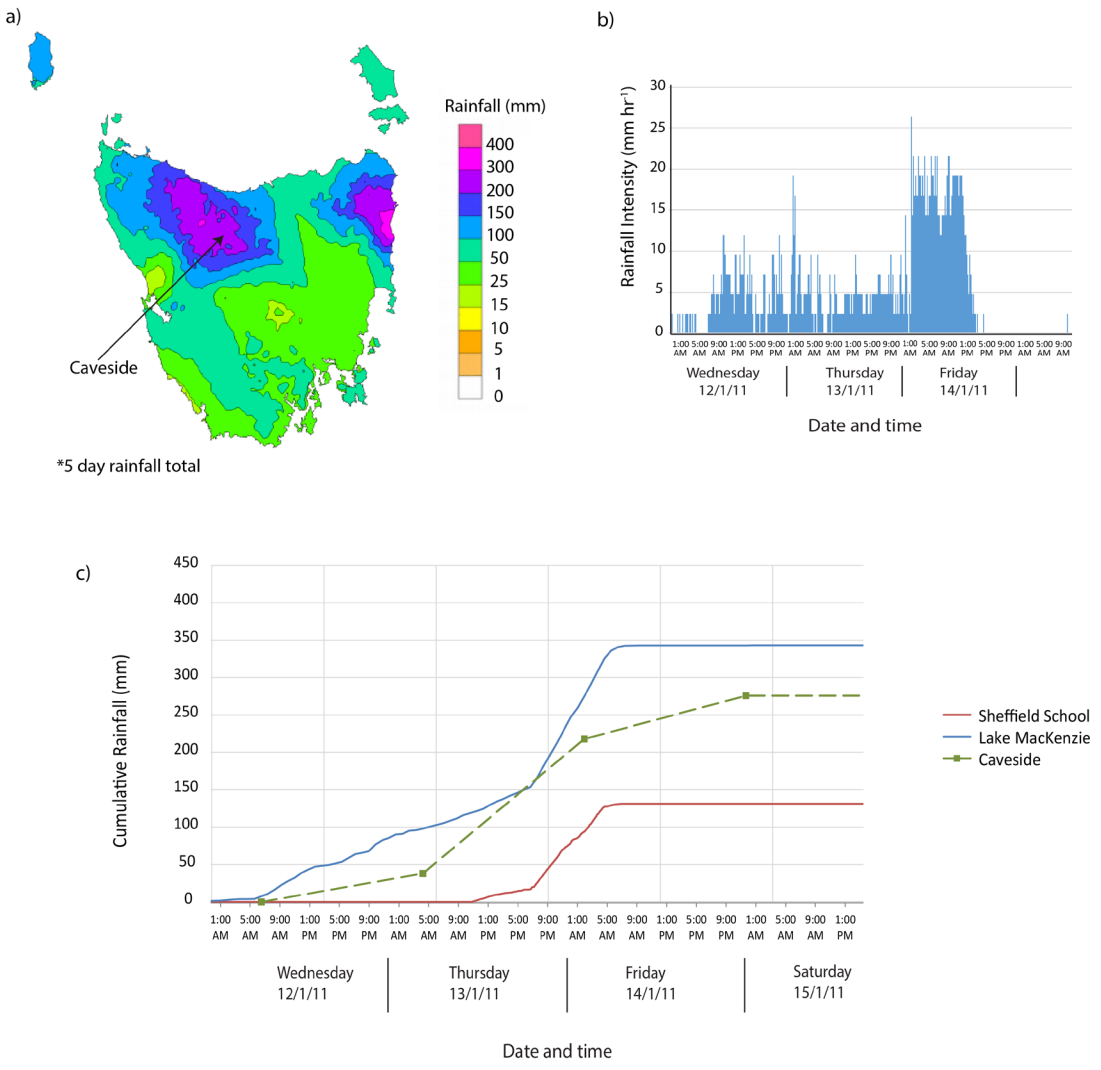

Figure 15. Rainfall data for the January 2011 storm. (a) 5-day rainfall total across Tasmania (BoM & ACSC, 2011); (b) hyetograph of rainfall at Lake Mackenzie; (c) cumulative rainfall at Caveside (daily totals) and the two nearest rainfall stations (continuous data).

the likely tolerance range of these estimated levels. At the three locations in the reach upstream of the farm buildings, where the simulated levels are more than 500 mm below the estimated levels, it is noted that each location was affected to some degree by debris blockage. It is also likely that part of the discrepancy between modelled and observed depths is due to the presence of fences on the properties, which were not included in the modelling inputs. Not only did the fences act as barriers that caused debris and flow to build up (visible in Fig. 13e), but debris marks on fences accounted for a large number of the calibration observations and this combination would have led to an overestimation of overall water elevations on the downstream flood plain. At the upper end of the farmland, the substantially higher observed water elevations are most likely due to a large pulse of floodwater that was witnessed by the landowners. Pulsing of water delivery (e.g., through log jam/debris dam generation and collapse) was not accounted for in the model.

A sensitivity test was performed, in which the Lake Mackenzie rainfall was run across the entire catchment and peak flood levels compared with those of the scaled rainfall scenario. Results confirmed that despite uncertainty in the actual distribution of rainfall on the catchment, varying rainfall between reasonable limits produces minimal change in peak flood levels.

Table 4. Peak flood levels. Observed levels were consistently higher than simulated values, although were generally within an acceptable tolerance level. The simulated levels at each location are shown in the column titled 'Computed Values' and the differences as 'Residual values'.

ID	Observed Value	Computed value	Residual value
1	366.7	365.804	-0.896
4	342.2	341.594	-0.606
6	349.9	349.681	-0.219
8	330.2	330.062	-0.138
10	328.5	327.968	-0.532
12	325	324.948	-0.052
13	319.7	319.339	-0.361
14	290.8	290.236	-0.564
15	311.7	311.381	-0.319
16	316.7	315.954	-0.746
17	299	298.802	-0.198
18	294.4	294.295	-0.105
19	294.7	294.93	0.23
20	289.9	289.952	0.052
21	290.1	289.736	-0.364
22	287.7	287.631	-0.069

The global use of the higher Lake Mackenzie rainfall generally produced an increase in flood levels of less than 10 mm.

January 2011

Rainfall

Unusually heavy rainfall was recorded across northern Tasmania between 12 January and 14 January 2011. This rainfall was generated by a trough of low pressure that brought moist air across Tasmania from the west (BoM & ACSC, 2011). The plot of total event rainfall extracted from BoM & ACSC (2011) shows Westmorland Stream again located in the centre of the highest rainfall zone in north-western Tasmania (Fig. 15a); a very similar spatial pattern to that of the 2016 event.

The storm exhibited an unusual rear-loaded rainfall pattern (Fig. 15b), whereby sporadic lower intensity rainfall occurred from 9:00 am on Wednesday 12 January to 1:00 am on Friday 14 January, before the bulk of the high intensity rainfall occurred in the final 12-hour period, on the morning of the 14 January. At Lake Mackenzie, 200 mm of precipitation was recorded in this 12-hour period, with a cumulative total of 340 mm covering the period from 12–14 January. A cumulative rainfall total of 180 mm was recorded at Sheffield School during this event (Fig. 15c). However, this value is significantly less than the daily recorded volumes at Caveside for this period, in contrast to the consistency observed in the 2016 event.

When plotted against the BOM IFD data for the Lake Mackenzie (Fig. 10), it can be seen that for shorter duration rainfall, burst intensities in the 2011 event were also relatively low (not rare), but again increase in rarity considerably as the burst duration approaches and exceeds 6 hours. The 2011 storm also exceeded a 1:100 AEP in the longer duration (6–48 hours) range, but it was not quite as rare as the 2016 event.

Landslides on the tiers above Caveside

Google Earth imagery acquired in March 2011 (approximately 2 months after the event) shows a landslide scar and a scoured zone that follows the path of Westmorland Stream (MRT Landslide ID 4840). Satellite imagery taken prior to January 2011 shows the stream was enclosed in forest canopy prior to the storm. When the landslide initiation location is mapped, it coincides with the boundary between the upper and lower Parmeener Group rocks and is situated at the headwaters of Westmorland Stream (Fig. 11). The stream bed was scoured from the landslide scar to a little beyond the forest boundary, covering a 2.9 km length and reaching a maximum width of 50 m. Large boulders, felled trees and log jams can be seen in the satellite imagery at numerous points within the channel. The forest area at the base of the hillside was filled with boulder debris, but the trees here largely remained standing. A smaller, contained landslide was also mapped from Google Earth imagery following this event (MRT Landslide ID 6345).

Patterns of erosion and deposition

The geomorphic impacts of the 2011 event were determined primarily from aerial imagery and the recollections of witnesses. No field investigation was undertaken at the time, but some impacts on the Westmorland Stream channel and the national park have been inferred from field observations in September 2016.

Geomorphic evidence of this event was still visible in the upper stream channel when field observations were undertaken in September 2016. Locals confirmed that this part of the hillside channel had not changed significantly following the 2016 flood (Noel Martin, pers. comm. 14 September 2016), and so the channel is largely representative of the conditions following the 2011 event. Park rangers report that the Westmorland Cave

interior remains blocked by large boulders and cobbles from the 2011 debris flow. Prior to the blockage, the cave entrance was large enough to walk through. As of 2016, the stream bed is still dominated by boulders and large log jams were observed in at least three locations.

Deposition patterns across the farmland were also mapped from Google Earth imagery (Fig. 16). Above the fan apex, deposition patterns were similar for the 2011 and 2016 events. Large lobes of gravel and boulder material were deposited across the flat area below the forest boundary. However, little erosion of alluvial material occurred and no significant scour zones were left following the 2011 flooding. From the top of the alluvial fan, mapping shows the main force of the 2011 event exited the constraints of the stream bed near the fan apex and tracked north along the boundary between the alluvial fan and the limestone hillside (Fig. 16), although some material was still transported down the stream channel. The landowners estimate that 2500 tonnes of material were deposited on the central part of the fan in 2011 (Mick Linger, pers. comm. 15 September 2016).

Video footage of the 2011 floodwaters at the upper part of the farmland show a high-velocity, sediment-laden flow. A single velocity calculation was possible from this record (date and time uncertain), which was taken at the location marked in Figure 17 and resulted in a value of approximately 2.1 ms^{-1}.

Reports from landowners suggest that the stream system also exhibited a more long-term response following the 2011 event. During historical times, the anthropogenically modified 9-foot channel and diversion chute have facilitated a continuous supply of fresh water down the alluvial fan and to the farms on the floodplain below. However, farmers report frequent water shortages during summer months between 2011 and 2016 and one witness described the water as disappearing into the gravel of the stream bed (Rodney Linger, pers. comm. 7 December 2016).

Flood modelling

The modelling results show a similar pattern of floodwater distribution as 2016; however, the volume of water and the duration of high-velocity, large-volume flow was significantly less. The outflow hydrograph shown in Figure 17 reflects the tail loaded rainfall pattern, with relatively constant high level discharges restricted to the tail end of the flood event. With a simulated peak outflow rate of about 55 m^3s^{-1}, the 2011 event outflow rate was not as high as that in the 2016 event and particularly high flowrates were restricted

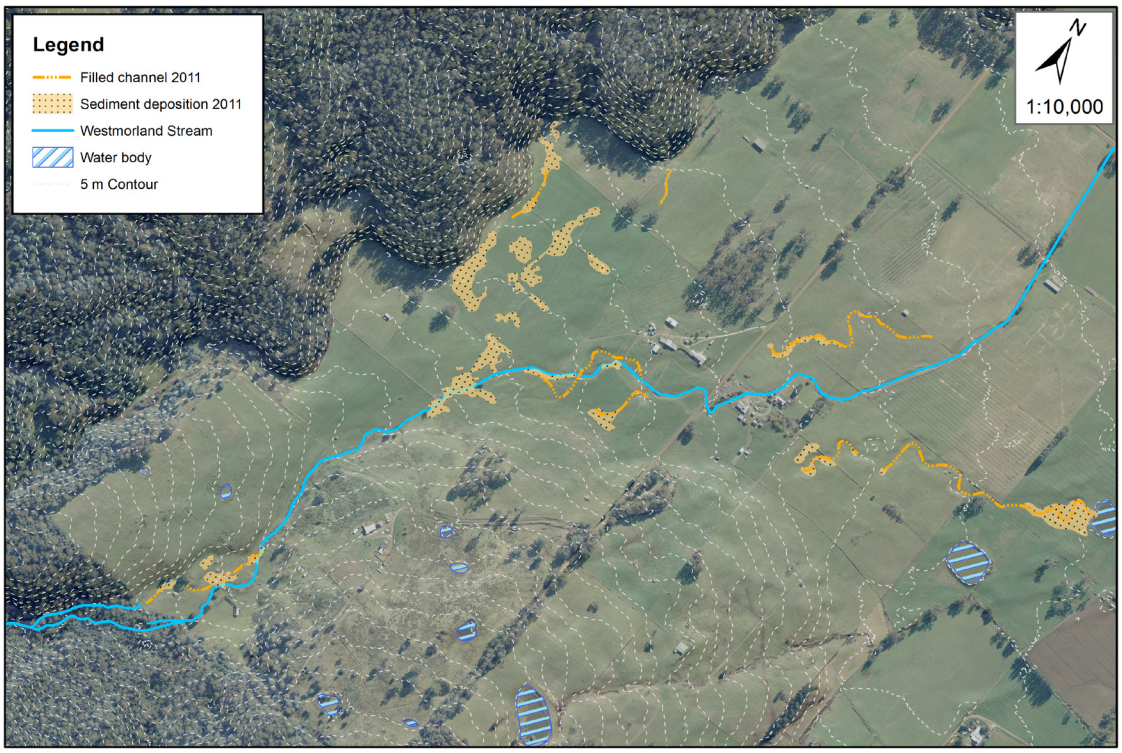

Figure 16. Patterns of erosion and deposition across the alluvial fan after the January 2011 event. Deposition was mapped from satellite imagery (Google Earth) taken in March 2011. Some clean-up had occurred between January and March, so the extent is known to be incomplete.

to the 12-hour period of intense rainfall at the tail end of the event. As a consequence, high stream velocities would have been for the most part only present during the last 12 hours of the event. However, velocities (as shown in Fig. 17) do persist at near peak level for most of that 12-hour period.

Interpretation and discussion

The alluvial fan and watershed

Mass movements, such as landslides and debris flows, are natural processes that are a common feature of the Tasmanian landscape. Landslides occur relatively frequently on the slopes of the GWT; however, it must be noted that an exceptional number were triggered around northern Tasmania during the June 2016 storm. Likewise, debris flows are also a common consequence of the geomorphology of the wider area. Historical records document several debris flows at the foot of the GWT (Anon, 1906), which appear to be similar to the events that occurred at Caveside.

Based on our observations, the alluvial fan at Caveside appears to be a composite-type that is formed by both debris flows and river floods through geological time, with a possible contribution from hyperconcentrated flows. It is interesting to note that no records of large floods transporting sediment, such as those in 2011 and 2016, have occurred since European settlement, and no rainfall events of these magnitudes are found in the historical rainfall data for Caveside.

a) Simulated flooding extent

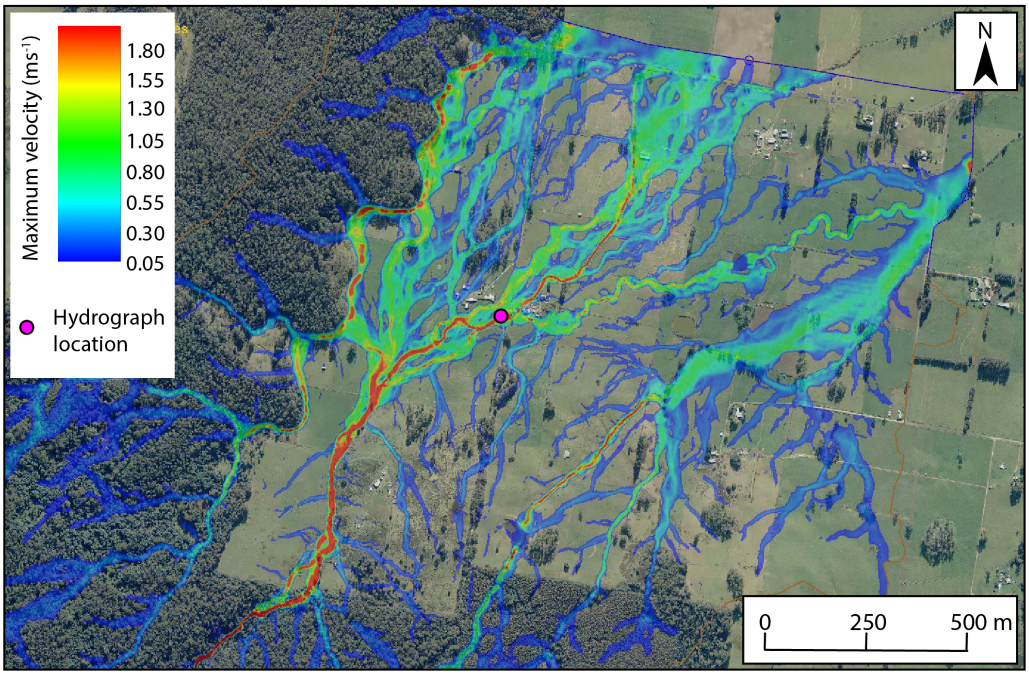

b) Outflow hydrograph

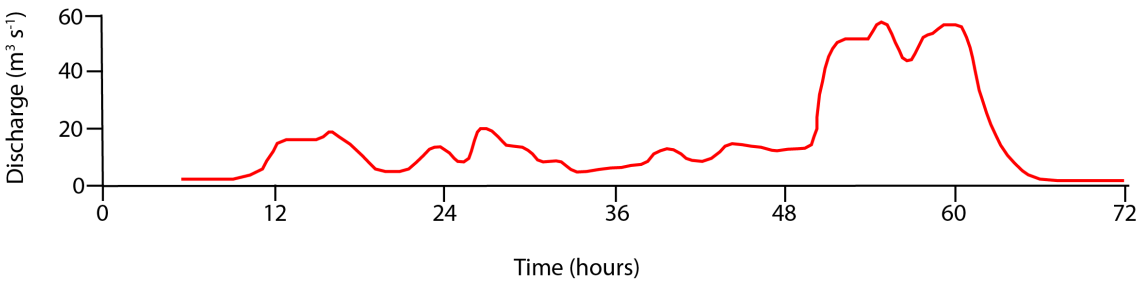

Figure 17. Results of hydraulic modelling for the 2011 event. (a) Flooding patterns and maximum velocities across the catchment and alluvial fan; (b) outflow hydrograph, showing modelled flood elevations in the Westmorland Stream channel on the upper part of the farmland.

We have not attempted to analyse the relative contribution of flooding and debris flows, deposition rates and natural climate cycles. Comparison of the morphometry of the Caveside watershed with the characteristics commonly associated with debris flow versus fluvial dominated fans (e.g., Wilford et al., 2004; de Scally et al., 2010; Santangelo et al., 2012) suggests that the study area is unlikely to be controlled by debris flow processes. The basin is comparatively large in area, long in length and gentle in gradient when compared to statistical studies of debris-flow fans (Table 3; Wilford et al., 2004; de Scally et al., 2010) and more closely aligns with the morphometric values obtained for fluvially dominated alluvial fans. In particular, the Melton Index of 0.33 strongly suggests the fan processes are currently fluvially dominated. However, the form and functioning of this system is somewhat complicated by the alluvial infilling of a confined valley area located at the base of the GWT (described as the 'upper farmland' in previous sections), before the stream exits onto the current fan apex. This area was included as part of the watershed feeding the active fan, as it technically occurs above the apex, but in reality this area exhibits the same inclination as the fan surface and acts as a 'catcher' for any debris flows that come from the steeper, true watershed behind. Despite this added complexity, the confined area is relatively small and does not substantially affect the morphometric calculations for the Caveside system.

The uppermost part of the GWT escarpment is prone to landslides along much of its length and the locations of these slips in relation to drainage channels (e.g., Westmorland Stream at Caveside as well as in a wider context) play a significant role in controlling the volume and method of sediment delivery to the fan systems below. This point will be discussed further in the following sections in relation to the 2011 and 2016 events.

Interpretation of processes during the 2016 and 2011 events

At face value, the impacts of the 2011 and 2016 events on the alluvial fan were similar and were initially considered to be a recurrence of the same processes. However, interpretation of the sediment deposits and comparison with modelled flow velocities suggests that the depositional mechanisms and sediment sources of these two events were different. These differences have implications for understanding the future flooding hazard and statistical frequency of recurrence. The 2011 event can best be described as a debris flow and flood combination that was related to a rainfall-triggered landslide at the top of Westmorland Stream, whereas the 2016 event was driven primarily by long-duration stream flooding and erosion of alluvium.

The nature of the sedimentary evidence and modelled flood velocities suggest the 2016 episode was primarily a stream flood, although some features of the deposits above the alluvial fan apex are indicative of localised debris flow processes. The combination of landslide scars and significant scouring on the western tributary stream suggests that a debris flow may have occurred down this stream during this event. However, satellite imagery shows that the stream bed remains enclosed in some places and large debris blockages are present along this stream as well as Westmorland Stream, which makes it difficult to determine what proportion and/or size fraction of this material reached the farmland below. In particular, Google Earth imagery shows that there is a build-up of material behind Westmorland Falls and far less scour in the bed below the falls, which suggests that much of the large material did not pass the falls. The timing of the two landslides on this stream is also difficult to determine. An area of closed canopy appears to be preserved immediately behind landslide 6352 (170 m upstream from Westmorland Falls), which could indicate that this slide occurred prior to landslide 6346 (at the headwaters of the tributary stream) and blocked the channel. This would imply that the scour took place in two separate phases.

The poorly sorted nature of the deposits on the upper farmland, and the presence of matrix-supported boulder beds, lobate features, levees, and undisturbed grass under the deposit toe are suggestive of a debris flow (Costa, 1988; Pierson, 2005a), that perhaps formed from a combination of runout material from the landslides on the tributary stream, as well as localised remobilisation of the 2011 material in the Westmorland Stream bed. Moreover, the failure of temporary dams (e.g., log jams) further upstream could have caused surges capable of moving this very coarse material short distances, as is common during mass movement processes in mountain gullies (Davies et al., 1992).

In contrast, the braided nature of the deposits and flood observations on the alluvial fan are more consistent with a stream flood (i.e., lower sediment concentrations and finer material). These deposits are more effectively sorted and contain a large proportion of vegetation debris, which is consistent with deposition from flow

with a lower sediment concentration (Costa, 1988). Furthermore, photographs suggest that the gravel and boulder deposits here are generally not matrix supported, with the finer material transported on to the floodplain below.

When comparing the volume of the channel scoured in the upper alluvial fan with the volume of deposited material, the values suggest that the deposited sediment was sourced primarily from erosion of alluvium at and immediately above the fan apex. Unlike the 2011 event, the stream bed of upper Westmorland stream was comprised mainly of boulders that are too large to be transported in suspension by water floods of the modelled magnitude. Consequently, the mountain stream bed can be discounted as the source of the coarse sediment lower down the catchment. However, finer material (silts and sands) resulting from the slips and scour on the GWT would likely have contributed to the fines deposited on the flood plain and lower alluvial fan. Model results show that flood velocities capable of eroding the alluvium (at times approaching 4 ms^{-1}) were maintained for 27 hours, which also accounts for the extreme amount of erosion that occurred.

The 2011 event differs from that of 2016 in that the upstream catchment was undisturbed prior to the scour that was initiated down the 2.9 km length of Westmorland Stream. In this case, a large influx of sediment was delivered to the top of Westmorland Stream in the form of a landslide, which then appears to have caused a debris flow that scoured the stream bed and deposited boulders and finer sediments as far as the upper part of the alluvial fan. The timing of events during 2011 is undocumented; however, the pattern of deposition on the fan itself again more closely resembles that of a flood deposit, rather than a debris flow. As the watershed had been undisturbed for a long period before this event, it seems likely that the debris flow provided a source of sediment that was then further transported by flooding during the final 12 hours of the event when the rainfall intensity was greatest. Little erosion of alluvium was observed during the 12 hours of intense flooding or in the days following (as seen in video footage and post-event aerial photographs), implying that erosion of the farmland was negligible as a sediment source during this flood.

The primary driver of process differences in 2011 and 2016 was most likely the occurrence of a large landslide and debris flow feeding into Westmorland Stream (in 2011), compounded by variation in rainfall patterns and duration between the two storms and the differences in antecedent morphology that resulted from the impacts of the 2011 event on the mountain part of Westmorland Stream. The volume of rain that fell above Caveside in 2016 was 30% higher than that of 2011, but most importantly, high intensity rainfall occurred over a longer period and high velocity (erosional) flow was maintained for a much longer period in 2016 than 2011. The flow paths across the farmland were different for the two events, with the main force of the 2011 event tracking north and the 2016 event largely following the stream channel east. These differences are a function of natural alluvial fan processes, by which channel avulsion and fan aggradation and progradation occurs during river floods.

Model limitations

Some limitations are inherent in the data acquisition and/or modelling process and must be acknowledged; however, it is unlikely that these compromise the quality of the results and their interpretation.

Firstly, mesh resolution in the main creek channel was set at 2 m. As such, some sections of narrow channel will not have been replicated in full detail. However, in major overbank flooding this would not impact peak flood elevations or velocities.

Topographic changes in 2011 due to landslips, debris flows, scour and deposition would have altered flood behaviour during the event to an unknown extent. The adopted topography in the 2011 modelling was that recorded (from the LiDAR survey) after the event and would incorporate not only the scour/deposition impacts from the event, but also include the impact of clean-up operations undertaken after the event. The potentially significant impact of landslips and debris flows on the timing of these changes may have been considerable. Flood behaviour simulated for this event is therefore of limited reliability but does serve to demonstrate the similarity of flood extents between 2011 and 2016, despite considerable differences in rainfall temporal patterns and intensities. Moreover, significant deposition on the floodplain (particularly upstream of fence lines) is likely to have elevated flood levels upstream of these areas relative to the modelled levels. Progressive channel scour and demolition of some structures would also have potentially lowered flood levels in these eroded areas relative to the modelled levels.

Debris dam failure in 2016 in the upper heavily forested reach seems very likely and would have significantly increased, for a short time, both the peak flow rate and associated flood levels, particularly in the vicinity of the more confined channel immediately downstream of the forest boundary. As there is no reliable data in respect to the location or geometry of this debris dam, it has not been included in the model. It would however seem to be the most likely reason why estimated peak flood levels on the pasture land are consistently higher than those simulated.

Uncertainties in spatial and temporal distribution of rainfall must be acknowledged, as the nearest continuous recording gauge is at Lake Mackenzie on the plateau of the Western Tiers, outside of the modelled domain. However, as daily rainfall was recorded at Caveside, a reasonably reliable estimate of the gradient in event rainfall could be established from the continuous rainfall at both locations. Therefore, this is not considered a significant limitation.

Future flooding hazard and implications

Processes and exceedance probabilities

The close timing of these two major events has been particularly distressing for the Caveside community. However, the occurrence of two major floods in a 6-year period is not extraordinary in a geomorphological context, particularly considering that both were initiated by unprecedented rainfall events. The total volume of rainfall for both events falls beyond the 1% AEP category (i.e., a storm with a 1:100 chance of occurring in any year; Fig. 6). However, in the case of mountain alluvial systems with a short response time and risk from either flash flooding and/or debris flows, it would be overly simplistic to quantify risk based on expected total rainfall volume alone.

It is important to note that flooding and erosion/deposition are two different processes that while frequently linked, may exhibit substantially different rarities. As such, the future hazard and recurrence rate must be considered with respect to intensity, duration and sediment availability. As yet, the rainfall thresholds for triggering flooding and mass movements around the GWT have not been explored, and this represents a pertinent area for further work in Tasmania (e.g., Caine, 1980; Guzzetti et al., 2008).

In considering the rarity of flooding (flow and level), it is the burst duration within the storm that controls flow, which in turn establishes the rarity of the resulting flood (Rigby et al., 2005). The IFD for the 2011 and 2016 storms (Fig. 6) shows that for burst durations in the range of 4 to 6 hours (the critical burst duration maximising flow: Rigby et al., 2005), both events incorporated bursts of 1:20 to 1:50 AEP. Assuming catchment antecedent conditions were average for such an event, the resulting flooding (independent of sediment transport processes) would be of comparable rarity. As such, both the 2011 and 2016 events were relatively major flood events but not as severe as that of a 1:100 AEP event. However, no design event flood modelling has been undertaken in this investigation and while both the 2011 and 2016 events involved major flooding, the 1:100 AEP design event would likely create higher flows and flood levels than present in these existing events. A study of design flood behaviour and risk management in this area would be useful to quantify the risk to the dwellings on the alluvial fan and floodplain. This is of particular concern as climate change may lead to more frequent severe rainfall events around Northern Tasmania in the future (White et al., 2010).

In contrast, it is the longer duration (6–24 hr) rainfall that maximises erosion and depositional volumes, i.e., the resulting 'geomorphic effectiveness' of an event in a given watershed (e.g., Costa, 1987; Wieczorek, 1987; Miller, 1990). As is apparent in Figure 6, longer duration rainfall in both the 2011 and 2016 events was substantially rarer than that of a 1:100 AEP event. As such, both events would be classified as extremely rare from a sediment movement viewpoint. This is of particular importance, as, in both cases, the impact of the sediment deposition presented a greater challenge for the community than the floodwaters. Moreover, debris flows are generally accepted to represent a greater hazard than flash floods (Hungr et al., 2001; Wilford et al., 2004; Welsh and Davies, 2011; Santangelo et al., 2012).

The results of the morphometric analysis and geomorphic investigations suggest that stream flooding is the dominant process in this catchment, as opposed to debris flows. This is an important distinction, because without the contribution of the debris flow during the 2011 event, the impacts would have been far less severe on the alluvial fan. Moreover, we cannot predict the recurrence of debris flow events in terms of statistical AEP's, as recurrence is controlled primarily by sediment availability. We consider a recurrence of a debris flow of comparative severity to that in 2011 to be unlikely in the near future, as the occurrence of these two floods has effectively stripped the mountain part of the streambed

of transportable sediment. However, the possibility of another landslide feeding into the channel remains.

Hydraulic hazard and system resilience

The ongoing safety of residents and dwellings is the primary concern. It is clear from flooding occurring in 2011 and in 2016 that while the habitable dwellings located in the study area appear to be constructed above the level of past flooding, residents are for some time surrounded by relatively hazardous floodwater, with no road access in or out and are therefore at some risk should anyone become injured and require treatment during a future flood event of similar or larger magnitude. One residential property is considered to be at particular risk. The stream passes beneath the driveway of this residence and between the house and a shed, which creates a significant safety risk during flash floods or flooding of larger magnitude. The dwelling is also located between the current artificial stream channel and two sinuous abandoned channels, which would have represented the stream's natural path at varying times prior to the construction of the 9-foot channel. These old channels were re-utilised by the flood waters, which provided some relief from the overflowing artificial channel that passes beneath the access way. Other dwellings in the area present less of an immediate flooding concern, as they are located further from the channel and/or are sited on raised parts of the landscape.

The impact of these events on the system's physical functioning must also be considered. Anecdotal reports from locals suggest that the system behaved quite differently following the 2011 event, and again following the 2016 flooding. Although a natural system response to perturbation, these changes present a management issue for the farmers who rely on a steady water supply. In particular, the enlargement of the channel by erosion appears to be contributing to a decreased system response time and thus a greater risk of flash flooding downstream. Conversely, in the dry summer months the increased channel width, open canopy and boulder-filled stream bed will result in more evaporation than would have been previously occurring when the stream was partly enclosed in the forest and formed a narrow meandering channel across the open farmland. This has implications for water supply in the dry summer months.

From an economic perspective, these two events have been devastating for local landowners and have highlighted the importance of developing economic and physical resilience with respect to farming infrastructure and pasture damage. The financial ramifications will not be discussed in this report, but there is a need for research into mechanisms for minimising the impact of potential future events and building resilience in case of further flooding. The hydraulic model constructed as part of this project may be useful as a tool for exploring future options and impacts.

Conclusions

The Westmorland Stream system has been affected by extreme flooding and sediment movement twice in a 6-year period. These events were both driven by large storms, with approximately 300 mm of rainfall delivered over 3 days in January 2011 and 400 mm over 3 days in June 2016. A combined investigative approach, which included field investigation, aerial imagery mapping and flood modelling, provided the means to determine the geomorphic mechanisms and sediment sources involved in these two events, as well as quantify risk from future events.

Both episodes involved the transportation and deposition of large amounts of sediment across the alluvial fan, but the processes involved in each were slightly different. The 2011 event was driven primarily by a landslide and debris flow on Westmorland Stream near the GWT escarpment, which scoured the mountain stream channel along a 2.9 km length and delivered sediment to the alluvial fan below in conjunction with severe flooding. These hillslope processes delivered a large volume of material to the system that was then mobilised downstream by flooding. In contrast, the impacts of the 2016 event were caused primarily by long-duration extreme flooding on the alluvial fan itself, where high velocity flow over a 27-hour period eroded over 3500 m^3 of material from the upper part of the farmland and moved it downstream.

Layers of coarse material visible in the eroded stream banks show that events such as these have formed the alluvial fan and are a natural part of the system. However, intensity-frequency-duration data suggests that storms of this magnitude (and consequently their severe impacts) have an annual exceedance probability of <1%, so a similar event is statistically unlikely to recur in the near future.

Both episodes had a devastating impact on the affected landowners and have altered the physical functioning

of the stream system, which has flow-on effects for land management. In particular, large-scale erosion has caused the stream to respond faster to rainfall events on the GWT and this presents a risk to farmers downstream. Conversely, the widened channel has also resulted in increased evaporation, which presents water scarcity issues in the summer months. These findings highlight the need to understand the risks from future events and develop ways to build economic and physical resilience in case of further events in the future.

Acknowledgements

Thank you to the local community members who kindly welcomed us into their homes, provided information and photographs of the floods and acted as guides: Ruth and Gavin Linger, Sally and Noel Martin, Julie and Wayne Paul, Rodney Linger and Nigel Linger.

We also wish to thank Peter Voller and Rob Buck (DPIPWE), Mark Willis (Meander Valley Council) for road information, and Hydro Tasmania for rainfall data.

References

Allen J. R. L. 1965. A review of the origin and characteristics of recent alluvial sediments. *Sedimentology* **5**: 89–191.

Anon. 1906. Terrific 'waterburst" on the "Woodside" estate of Mr Basil Archer, Cressy district, northern Tasmania. *The Weekly Courier* (Launceston, Tasmania), Saturday October 27 1906: 20–21, 34.

Bull W. B. 1977. The alluvial fan environment. *Progress in Physical Geography* **1**: 222–270.

Bureau of Meteorology Tasmania and Antarctica Climate Services Centre (BoM & ACSC) 2011. *Heavy rainfall and flooding in northeast Tasmania*. Special Climate Statement 30.

Bureau of Meteorology (BoM) 2016a. Climate Data Online. http://www.bom.gov.au/climate/data/. Accessed 7 September 2016.

Bureau of Meteorology (BoM) 2016b. Special Climate Statement 57 – extensive early June rainfall affecting the Australian east coast. http://www.bom.gov.au/climate/current/statements/scs57.pdf. Accessed 27 September 2016.

Bureau of Meteorology (BoM) 2016c. Rainfall Intensity-Frequency-Duration (IFD) Data System. http://www.bom.gov.au/water/designRainfalls/revised-ifd/?. Accessed 7 September 2016.

Caine N. 1980. The rainfall intensity-duration control of shallow landslides and debris flows, *Geografiska Annaler* 62A: 23–27.

Calvache M. L.; Viseras C.; Fernández, J. 1997. Controls on fan development—evidence from fan morphometry and sedimentology; Sierra Nevada, SE Spain. *Geomorphology* **21**: 69–8

Corbett K. D.; Quilty P. G.; Calver C. R. 2014. *Geological Evolution of Tasmania*. Geological Society of Australia, Tasmania Division.

Costa J. E. 1984. Physical geomorphology of debris flows. *In* Costa J.E. & Fleisher P.J., (Eds), *Developments and Applications of Geomorphology*. Springer, Berlin: 268–317.

Costa J. E. 1987. Hydraulics and basin morphometry of the largest flash floods in the conterminous United States. *Journal of Hydrology* **93**: 313–338.

Costa J. E. 1988. Rheologic, geomorphic, and sedimentologic differentiation of water floods, hyperconcentrated flows, and debris flows. *In* Baker V. R.; Kochel R. C.; Patten P. C. (Eds) *Flood Geomorphology,* Wiley-Intersciences, New York: 113–122.

Crosta G. B.; Frattini P. 2004. Controls on modern Alluvial fan processes in the Central Alps, Nothern Italy. *Earth Surface Processes and Landforms* **29**: 267–293.

Davies T. R.; McSaveney M. J. 2008. Principles of sustainable development on fans. *Journal of Hydrology* (New Zealand) **47**: 43–65.

Davies, T. R.; Phillips C. J.; Pearce A. J.; Zhang X. B. 1992. *Debrisflow behaviour—an integrated overview*. International Association of Hydrological Sciences Publication 209: 217–225.

de Scally F. A.; Owens I. F. 2004. Morphometric controls and geomorphic responses on fans in the Southern Alps, New Zealand. *Earth Surface Processes and Landforms* **29**: 311–322.

de Scally F. A.; Owens I. F.; Louis J. 2010. Controls on fan depositional processes in the schist ranges of the Southern Alps, New Zealand, and implications for debris-flow hazard assessment. *Geomorphology* **122**: 99–166.

de Scally F.; Slaymaker O.; Owens I. 2001. Morphometric controls and basin response in the Cascade Mountains. *Geografiska Annaler* **83A**(3): 117–130.

Guzzetti F.; Peruccacci S.; Rossi M.; Stark C. P. 2008. The rainfall intensity–duration control of shallow landslides and debris flows: an update. *Landslides* **5**: 3–17.

Harvey A.; Mather A. E.; Stokes M. 2005. Alluvial fans: geomorphology, sedimentology, dynamics-introduction, a review of alluvial fan research. *In* Harvey A., Mather A. E. & Stokes M. (Eds), *Alluvial fans: geomorphology, sedimentology, dynamics.* Geological Society Special Publication 251, London: 1–8.

He Y. P.; Xie H.; Cui P.; Wei F. Q.; Zhong D. L.; Gardner J. S. 2003. GIS-based hazard mapping and zonation of debris flows in Xiaojiang Basin, southwestern China. *Environmental Geology* **45**: 286–293.

Hjulström F. 1935. Studies of the morphological activity of rivers as illustrated by the River Fyris. *Bulletin of the Geological Institute of the University of Uppsala* **25**: 221–527.

Hungr O. 2005. Classification and terminology. In: Jakob M.; Hungr & O. (Eds), *Debris-Flow Hazards and Related Phenomena.* Praxis Springer, Berlin: 9–23.

Hungr O.; Morgan G. C.; Kellerhals R. 1984. Quantitative analysis of debris torrent hazards for design of remedial measures. *Canadian Geotechnical Journal* **21**: 663–677.

Hungr O.; Evans S. G.; Bovis M. J.; Hutchinson J. N. 2001. A review of the classification of landslides of the flow type. *Environmental and Engineering Geoscience* **7**(3): 221–238.

Hunter D. 2011. Recent changes in the local hydrology, Lobster Rivulet catchment, Mole Creek karst: The landslides of January 2011. *Proceedings, Cave and Karst Management in Australasia* 19, Ulverstone Tasmania, May 2011.

Hydronia LLC 2016. RiverFlow2D Two-Dimensional River Dynamics Model, Reference Manual. http://www.hydronia.com/ Accessed 15 January 2017.

Jakob M.; Hungr, O. (Eds) 2005. *Debris-Flow Hazards and Related Phenomena*. Springer, Berlin.

Jennings I. B.; Burns K. L. 1958. Middlesex. 1:63360. Geological Atlas 1:50 000 series. Tasmania Department of Mines.

Kiernan K. 1995. *An Atlas of Tasmanian Karst*. Research Report No. 10, Tasmanian Forest Research Council, Tasmania.

Kostaschuk R. A.; MacDonald G. M.; Putnam P. E. 1986. Depositional process and alluvial fan-drainage basin morphometric relationships near Banff, Alberta, Canada. *Earth Surface Processes and Landforms* **11**: 471–484.

Lorente A.; García-Ruiz J. M.; Beguería S.; Arnáez, J. 2002. Factors explaining the spatial distribution of hillslope debris flows: a case study in the flysch sector of the central Spanish

Pyrenees. *Mountain Research and Development* **22**: 32–39.
McIntosh P. D.; Eberhard R.; Slee A.; Moss P.; Price D. M.; Donaldson P.; Doyle R.; Martins J. 2012. Late Quaternary extraglacial cold-climate deposits in low and mid-altitude Tasmania and their climatic implications. *Geomorphology* **179**: 21–39.
Melton M. A. 1965. The geomorphic and paleoclimatic significance of alluvial deposits in southern Arizona, *Journal of Geology* **73**: 1–38.
Miller A.J. 1990. Flood hydrology and geomorphic effectiveness in the Central Appalachians. *Earth Surface Processes and Landforms* **15**: 119–134.
National Research Council (NRC) 1996. *Alluvial Fan Flooding*. National Academy Press, Washington, DC. 131 pp.
Norini G.; Zuluaga M. C.; Ortiz I. J.; Aquino D. T.; Lagmay A. M.F. 2016. Delineation of alluvial fans from Digital Elevation Models with a GIS algorithm for the geomorphological mapping of the Earth and Mars. *Geomorphology* **273**: 134–149.
Pierson T. C. 2005a. Distinguishing between debris flows and floods from field evidence in small watersheds. *USGS Fact Sheet* 2004–3142.
Pierson T. C. 2005b. Hyperconcentrated flow – transitional process between water flow and debris flow. *In* Jakob M.; Hungr O. (Eds), *Debris-Flow Hazards and Related Phenomena.* Praxis Springer, Berlin: 159–202.
Pierson T. C.; Costa J. C. 1987. A rheologic classification of sub-aerial sediment-water flows. *In* Costa J. E.; Wieczorek G. F. (Eds), Debris Flows/Avalanches: Process, Recognition and Mitigation, *Geological Society of America Reviews in Engineering Geology* **7**: 1–12.
Rigby T.; Boyd M.; Roso S.; VanDrie R. 2005, Storms, store bursts and flood estimation: A need for review of the AR&R procedures, *Australian Journal of Water Resources* **8**(2): 213–222.
Santangelo N.; Daunis-i-Estadella J.; Di Crescenzo G.; Di Donato V.; Faillace P.; Martin-Fernandez J. A.; Romano P.; Santo A.; Scorpio V. 2012. Topographic predictors of susceptibility to alluvial fan flooding, Southern Apennines. *Earth Surface Processes and Landforms* **37**: 803–817.
Sorriso-Valvo M.; Antronico L.; Le Pera E. 1998. Controls on modern fan morphology in Calabria, southern Italy. *Geomorphology* **24**: 169–187.
Takahashi T. 2007. *Debris Flow Mechanics, Prediction and Countermeasures*. Taylor & Francis, 440 pp.
Wasson R. J. 1977. Last-glacial alluvial fan sedimentation in the Lower Derwent Valley, Tasmania. *Sedimentology* **24**: 781–800.
Welsh A.; Davies T. 2011. Identification of alluvial fans susceptible to debris flow hazards. *Landslides* **8**: 183–194.
White C. J.; Grose M. R.; Corney S. P.; Bennett J. C.; Holz G. K.; Sanabria L. A.; McInnes K. L.; Cechet R. P.; Gaynor S. M.; Bindoff N.L. 2010. *Climate futures for Tasmania: extreme events technical report*. Antarctic Climate and Ecosystems Cooperative Research Centre, Hobart, Tasmania.
Wieczorek G. F. 1987. Effect of rainfall intensity and duration on debris flows in central Santa Cruz mountains, California. *Reviews in Engineering Geology* **7**: 93–104.
Wilford D. J.; Sakals M. E.; Innes J. L.; Sidle R. C.; Bergerud W. A. 2004. Recognition of debris flow, debris flood and flood hazard through watershed morphometrics. *Landslides* **1**: 61–66.